Appendix F15

Duncan 2014

Prediction of Underwater Noise Levels associated with the Operation of FLNG facilities in the Browse Basin

BROWSE FLNG DEVELOPMENT
Draft Environmental Impact Statement

EPBC 2013/7079
November 2014

Curtin University

Centre for Marine Science and Technology

Prediction of underwater noise levels associated with the operation of FLNG facilities in the Browse Basin

DRAFT

Prepared for:

Sinclair Knight Mertz

Prepared by: Alec Duncan
Reviewed by:
PROJECT CMST 1280
REPORT 2014-12

15th April 2014

Executive Summary

This report presents the results of modelling of the production and propagation of underwater noise associated with the operation of Floating Liquefied Natural Gas (FLNG) processing and storage facilities in the Browse basin off the northwest coast of Australia.

Received underwater noise levels from FLNG facilities operating in the Torosa and Brecknock/Calliance fields have been modelled.

FLNG source spectra were estimated by scaling measured underwater noise spectra from existing Floating Production Storage and Offloading (FPSO) facilities, which indicated there would be an approximately 10 dB difference between mean and maximum noise levels from each FLNG facility during normal operations. The additional thruster cavitation noise present during offloading operations substantially increases the received noise levels above the mean FLNG operational noise, but only marginally increases it above the maximum FLNG operational noise.

Modelling shows that sound from the Torosa facility is unable to penetrate into the North Reef lagoon but can penetrate the South Reef lagoon along some azimuths, due to the relatively deep sill along the northern boundary of this lagoon.

The report details the resultant modelled sound fields for different operating scenarios.

Table of Contents

List of Figures

List of Tables

1 Introduction

This report presents the results of numerical modelling of the production and propagation of underwater noise associated with the operation of Floating Liquefied Natural Gas (FLNG) facilities in the Browse basin off the northwest coast of Australia.

This report deals with proposed FLNG facilities in the Torosa and Brecknock/Calliance fields. The Torosa facilities are a few kilometres east of Scott Reef, and the Brecknock/Calliance facilities are about 40 km to the southwest of the reef. The regional location is shown in Figure 1. The locations of proposed FLNG facilities are shown in Figure 2 (Torosa) and Figure 3 (Brecknock/Calliance). The initial development will comprise two FLNG facilities (BWA and BWB) at Brecknock/Calliance and one (BWC) at Torosa. The facility at BWB may be relocated to Torosa in the future where it is named BWB-TR.

Scott Reef consists of two coral atolls separated by a narrow channel. There is a third atoll, Seringapatam Reef, also visible in Figure 2, some distance to the north. These atolls rise steeply from the surrounding seafloor which is at a depth of about 400m. Water depths on the reefs vary between essentially zero to approximately 60m (see Figure 4).

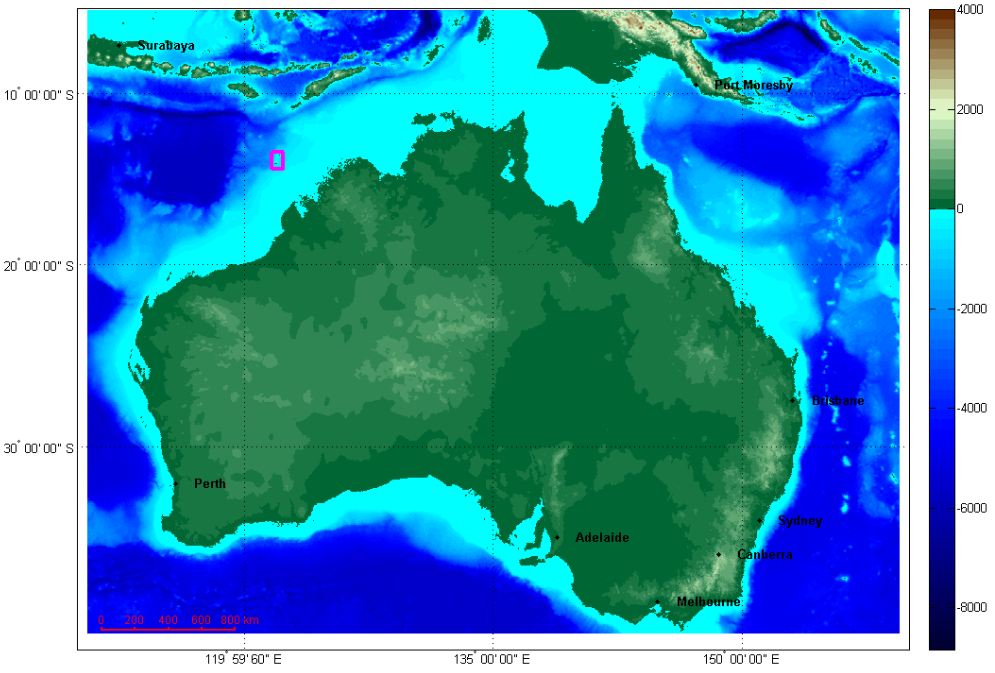

Figure 1. General location map. The magenta rectangle off the northwest coast of Australia is the region shown in subsequent plots.

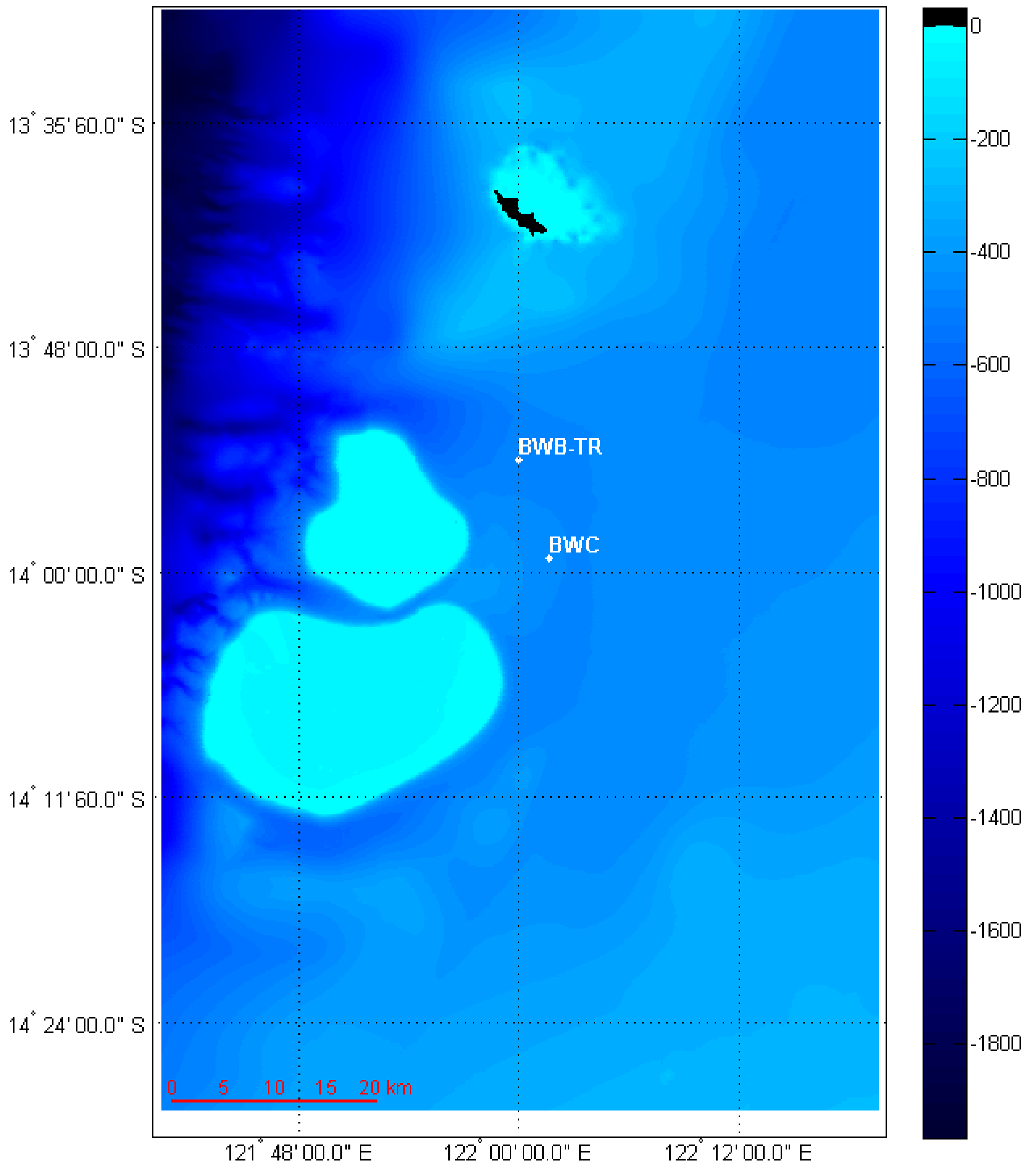

Figure 2. Bathymetry in the vicinity of the proposed Torosa FLNG locations (white points labelled BWC and BWB-TR).

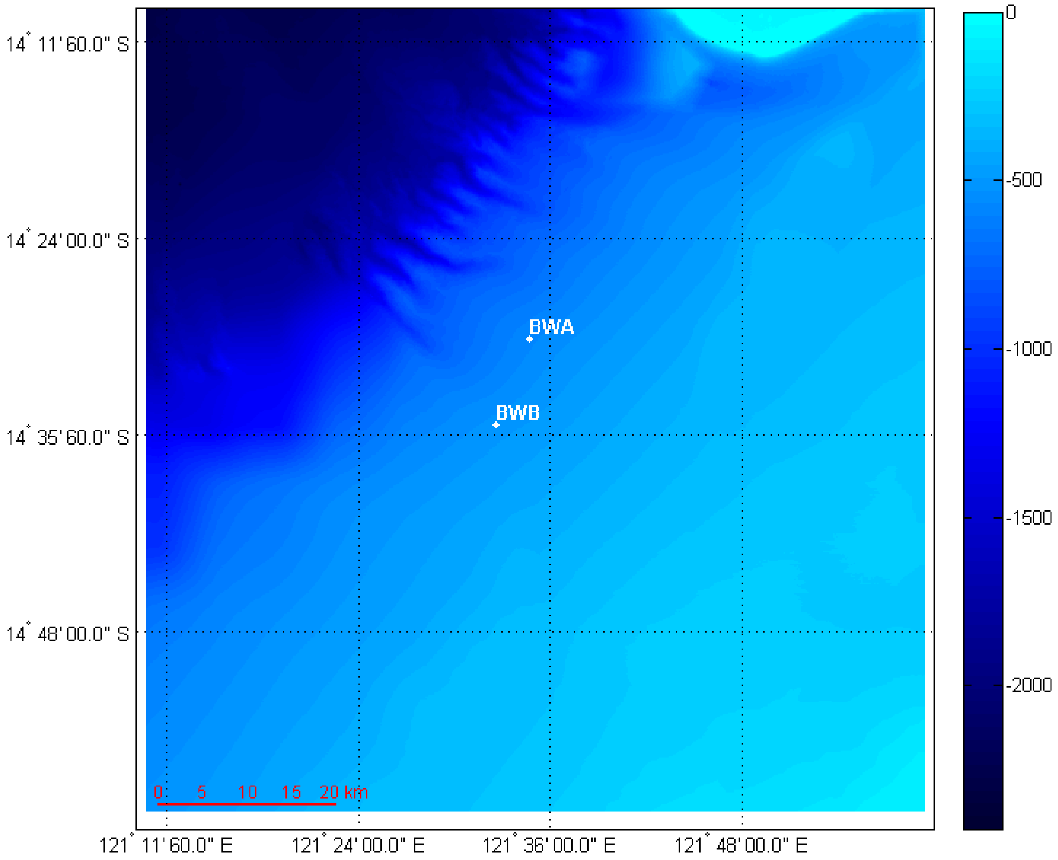

Figure 3. Bathymetry in the vicinity of the proposed Brecknock/Calliance FLNG locations. Scott Reef South is just visible in the top right of the plot.

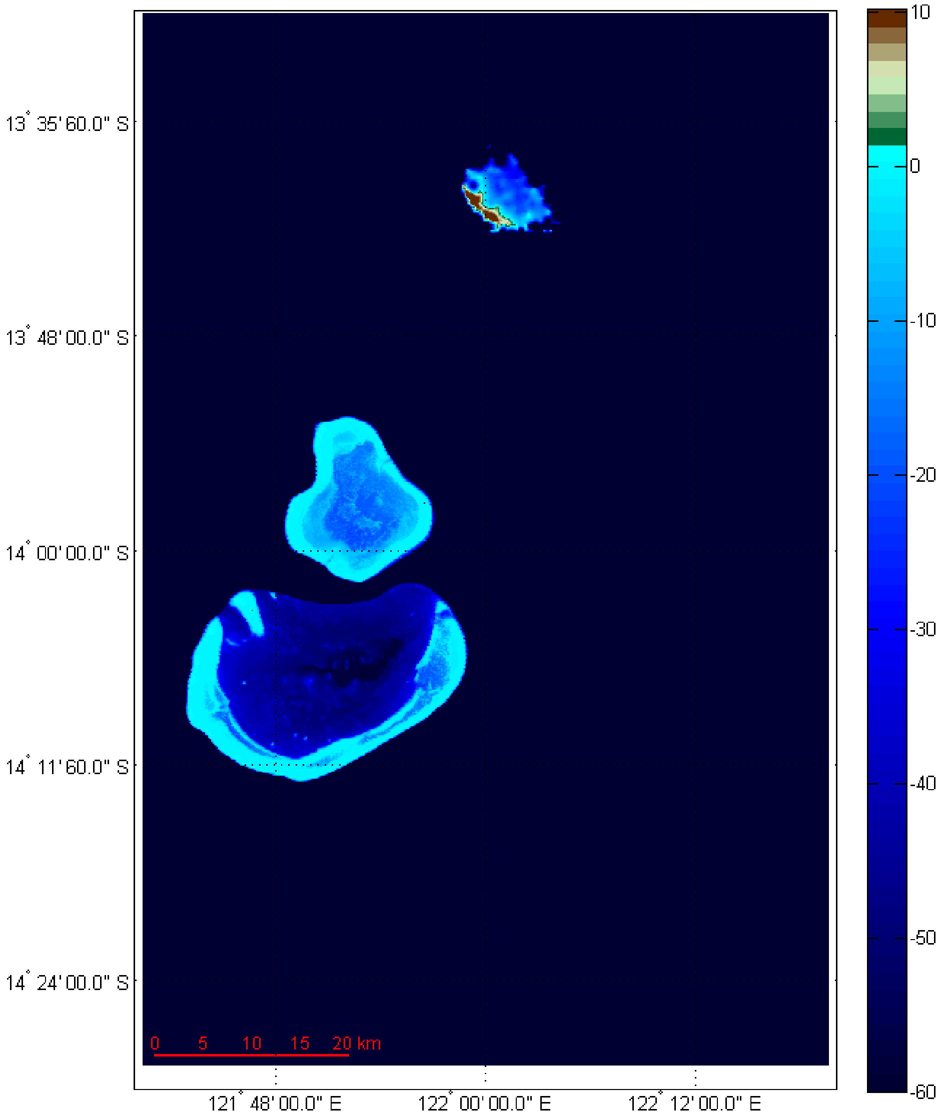

Figure 4. Bathymetry showing only depths to 60m.

2 Methods

2.1 Acoustic source spectra

FLNG facility noise during normal operations

In the absence of any measurements of underwater noise from FLNG facilities, acoustic source spectra for the FLNG facility during normal operations were based on generic Floating Production Storage and Offloading (FPSO) facility source spectra derived by CMST from measurements made of underwater noise from three different FPSOs. Although generally smaller, FPSOs have a similar configuration to FLNGs, with much of the specialised processing machinery mounted above the main deck, and the electrical power generation machinery being located in the hull. FPSO noise is thus a reasonable starting point for estimating noise from a FLNG.

The FPSO measurements showed large variations both between vessels and over time for a single vessel, so two spectra were derived: a mean spectrum and a maximum spectrum. The mean spectrum was obtained by averaging over time for each vessel, and then averaging these results across vessels. (All averaging was carried out in the pressure squared domain.) The derived maximum spectrum is the upper envelope of all the measured spectra. These spectra are shown by the broken lines in Figure 5.

The larger size of the FLNG facility was accounted for by scaling the spectra on the theoretical assumption that the radiated acoustic power is a constant fraction of the installed electrical generation capacity of the vessel. Using an estimated FLNG total facility power (provided by Woodside) of 190 MW, and a typical FPSO power generation capacity of 20 MW results in a 9.8 dB offset of the FLNG facility source spectra relative to the corresponding FPSO spectra (see Figure 5). The corresponding broadband source levels calculated from these spectra (20 Hz to 1 kHz) are 192.1 dB re 1µPa rms @ 1m for the mean machinery noise and 201.1 dB re 1µPa rms @ 1m for the maximum machinery noise. Note that these broad-band source level values should be treated with caution as they are dominated by high spectral levels at very low frequencies (see Figure 5). This low frequency sound will be strongly attenuated by destructive interference between the direct and surface reflected paths and will not contribute significantly to the received signal at long range.

The source depth for propagation calculations was chosen to be 10m, which is close to half the draft of the fully laden vessel (19.5m).

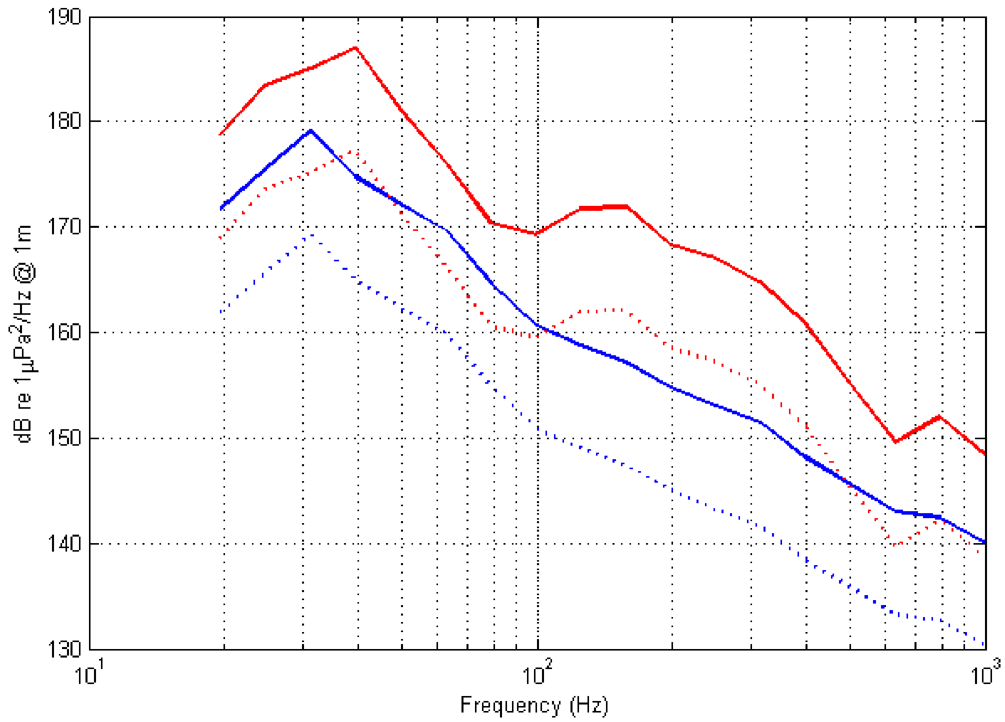

Figure 5. FPSO machinery noise source spectra. Dotted blue line is generic FPSO mean source spectrum and dotted red line is generic FPSO maximum source spectrum. Solid lines are the corresponding predicted mean and maximum FLNG facility source spectra obtained by offsetting the corresponding FPSO spectra by 9.8 dB.

Noise produced during LNG carrier berthing

The highest underwater noise levels produced during the operation of this facility are expected to occur during the berthing of the LNG carrier that will offload the LNG. Such operations are likely to involve the simultaneous operation of thrusters on the FLNG facility (to control its heading), thrusters on two high performance offshore support tugs, and the main engine of the LNG carrier. Thrusters on the FLNG facility and tugs will be generating high levels of thrust in poor flow conditions, resulting in significant propeller cavitation and consequent high underwater noise levels. Conversely the LNG carrier's propulsion system will be operating at low and fairly constant revolutions per minute, making propeller cavitation unlikely. The LNG carrier and tugs will also produce machinery noise, but this will be well below the cavitation noise from the thrusters on the FLNG facility and tugs, and has consequently not been included in the modelling. This noise will be in addition to the FLNG facility operational noise described above.

Because of its importance for passive sonar detection of ships and submarines, cavitation noise has been extensively studied, however this has been in the context of ships travelling at cruising speed, rather than ships and tugs manoeuvring at low speed. The source model used in this report is therefore based on measurements made by CMST of underwater sound levels produced by a rig tender (*Pacific Ariki*) while using its propulsion system to remain stationary near an offshore platform (McCauley 1998). The characteristics of the *Pacific Ariki* are given in Table 1, and the measured, one-third octave source spectrum is shown in Figure 6. Levels have been extrapolated to those to be expected for other vessels by assuming that a constant proportion of the mechanical power is converted to acoustic power. This relationship has been found to hold reasonably well for surface vessels operating at their normal cruising speed (Ross 1987). The resulting source spectra are also shown in Figure 6, and peak in the frequency range 200 to 400 Hz. The corresponding broadband source levels over 10 Hz to 2 kHz were calculated to be 188.9 dB re 1 μPa @ 1 m for the FLNG facility, and 189.7 dB re 1 μPa @ 1 m for the combined effect of the two tugs.

This *Pacific Ariki* spectrum is based on measurements made in a single direction relative to the vessel and therefore no source directionality data is available, however there was a clear path between the vessel's thrusters and the hydrophone. Given the nature of cavitation noise, and the fact that the thrusters are located at different positions on the vessel, and in many cases can be rotated in azimuth, it is reasonable to assume that it is omni-directional.

The FLNG facility cavitation noise was modelled as a point source at a thruster depth of 19.5 m, and the combined effect of the two tugs was modelled as a single source at a depth of 7 m. Received levels were calculated separately for the FLNG facility and the tugs, and the resulting mean-squared pressures were then summed.

Table 1. Characteristics of the *Pacific Ariki*

Vessel	Pacific Ariki
Length Over All	64 m
Operating draft	6.6 m
Tonnage	2,600 (displacement)
Propulsion power	4 x 1.5 MW = 6.0 MW
Retractable thrusters	1 x 0.6 MW
Tunnel thrusters	2 x 0.6 MW = 1.2 MW
Total thruster power	1.8 MW
Thruster plus propulsion power assuming 2 out of 4 main engines in use	4.8 MW
Measured broadband source level (10 Hz to 2 kHz)	185.7 dB re 1 μPa @ 1 m

Table 2. Assumed thruster powers and resulting source level corrections

Vessel	Pacific Ariki	FLNG facility	2 x Offshore support tugs
Installed thruster power	4.8 MW (tunnel thrusters plus 2 of 4 main engines)	10 MW (two thrusters in use)	12 MW (assumes each tug has two out of three thrusters in use)
Installed thruster power relative to Pacific Ariki	1	2.1	2.5
Source level correction	0 dB	3.2 dB	4.0 dB
Equivalent broadband source level (10 Hz to 2 kHz)	185.7 dB re 1μPa @ 1 m	188.9 dB re 1 μPa @ 1 m	189.7 dB re 1 μPa @ 1 m
Assumed source depth	6 m	19.5 m	7 m

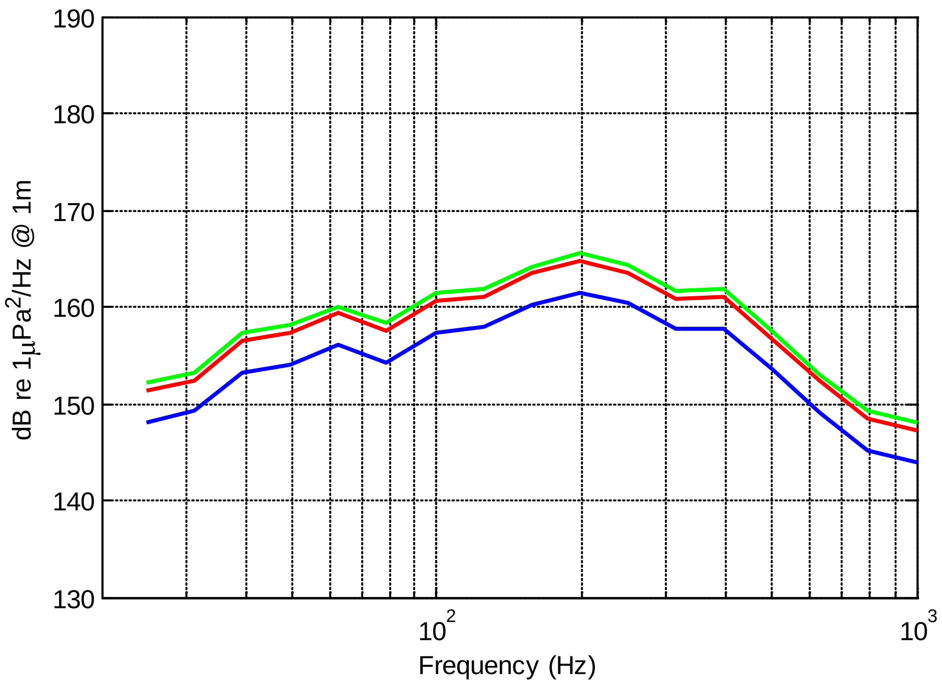

Figure 6. Cavitation noise source spectra. Blue line is measured source spectrum of the Pacific Ariki using its propulsion system to remain stationary near an offshore platform, red line is the predicted source spectrum for the FLNG facility thrusters, and green line is the predicted combined source spectrum for two ocean-going tugs.

2.2 Seabed geoacoustic model

Seabed geoacoustic models for the Torosa field were based on seabed descriptions given in Section 5 of the Browse - Torosa Development Geotechnical Condition Overview (DRIMS 7656141). This resulted in the modelling area being divided into three distinct seabed types which were designated: continental slope, reef, and reef debris. The region boundaries are shown in Figure 7.

Except in the immediate vicinity of the reefs, the seabed was modelled using a silt seabed typical of the continental slope at these water depths (see Table 3 for geoacoustic parameters). Parameter values at the water-silt interface were taken from Jensen et. al. (2011), and the depth dependencies of compressional wave speed and density were based on Hamilton (1979) and Hamilton (1976) respectively. From theoretical considerations of the attenuations involved, little or no energy would be expected to return to the water column from depths in the seabed of more than 200m so the seabed below this was modelled as a half-space with the same properties as at 200m.

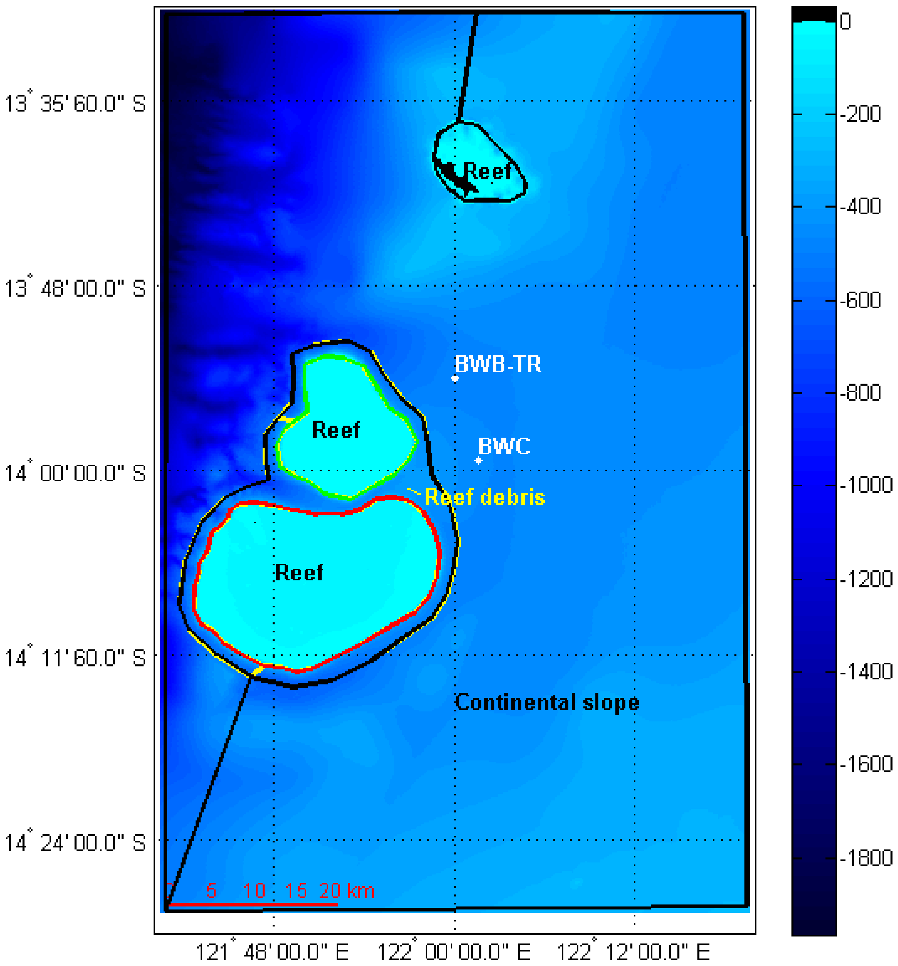

Figure 7. Geoacoustic region boundaries used for Torosa field modelling

Table 3. Geoacoustic properties for the continental slope seabed.

Depth in seabed (m)	**Compressional wave speed (m/s)**	**Density (kg/m^3)**	**Compressional wave attenuation (dB per wavelength)**
0	1566	1700	1
50	1627	1750	1
100	1686	1800	1
150	1742	1850	1
>200	1795	1900	1

The immediate surroundings of the reefs were modelled using parameters typical of coarse sand/gravel (Jensen et. al. 2011) which was considered reasonably representative of reef debris. The corresponding geoacoustic parameters are listed in Table 4.

The reefs themselves were modelled as limestone. Limestone is an elastic solid that supports both shear and compressional waves, which causes problems for acoustic propagation models. It was therefore modelled as an equivalent fluid, with the geoacoustic parameters of the fluid chosen to provide the best match between its plane wave reflection coefficient and that of the solid at the low grazing angles important for acoustic propagation in the water column. The low grazing angle approximation is not completely accurate in rugged terrain such as around Scott Reef but, in the opinion of the author, this is the best that can be done with currently available acoustic propagation models, and the use of this approximation is unlikely to have a significant effect on the results. The geoacoustic parameters for limestone were taken from Jensen et. al. (2011) and are listed in Table 5 together with those of the equivalent fluid that was used for modelling. In this case the parameters were assumed to be independent of depth into the seabed.

The seabed geomorphology in the vicinity of the Brecknock/Calliance facilities is described in the Browse Basin Geohazard Assessment (DRIMS 7207491) and is sufficiently uniform that the continental slope seabed properties given in Table 3 could be used throughout.

Table 4. Geoacoustic parameters used for the reef debris regions.

Depth in seabed (m)	**Compressional wave speed (m/s)**	**Density (kg/m^3)**	**Compressional wave attenuation (dB per wavelength)**
0	1714	1800	0.6
50	1782	1850	0.6
100	1847	1900	0.6
150	1908	1950	0.6
>200	1967	2000	0.6

Table 5. Geoacoustic parameters used for the reef regions.

Material	Density ($kg.m^{-3}$)	Compressional wave speed (m/s)	Compressional wave attenuation (dB per wavelength)	Shear wave speed (m/s)	Shear wave attenuation (dB per wavelength)
Limestone	2400	3000	0.1	1500	0.2
Equivalent fluid	2400	1350	14	-	-

2.3 Water column sound speed profile

The water-column sound speed profile was taken from the nearest grid point of the World Ocean Atlas (2005) for the southern hemisphere summer and is shown in Figure 8.

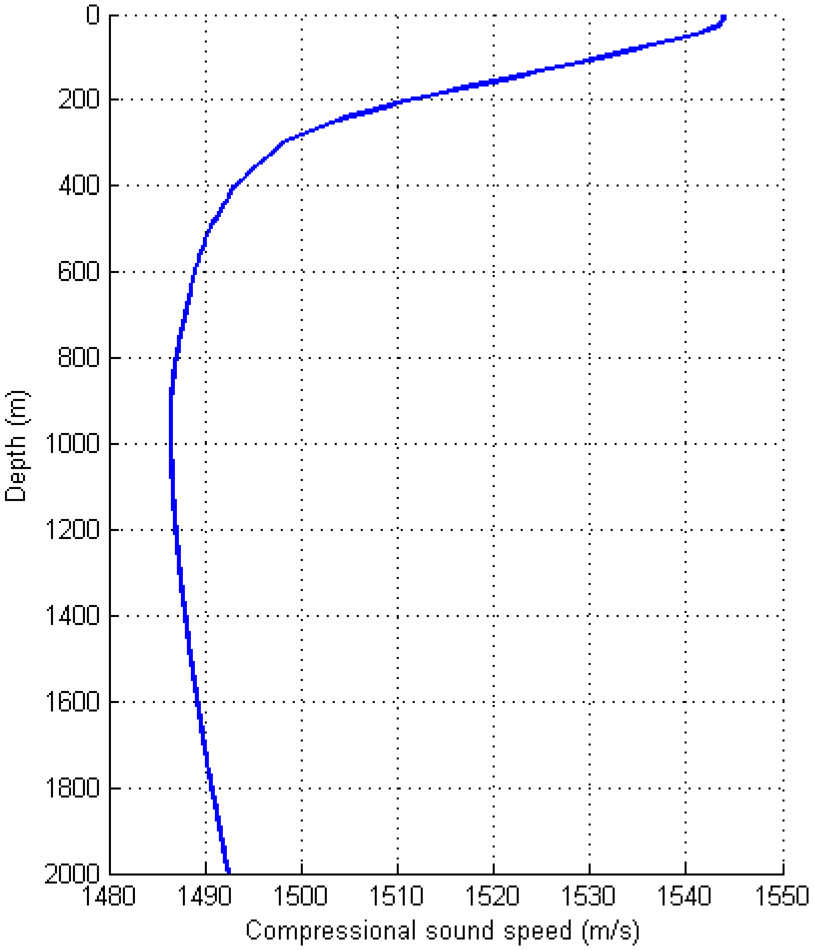

Figure 8. Sound speed profile used for modelling.

2.4 Acoustic propagation modelling and received level calculation

The acoustic propagation model RAMGeo was used to calculate transmission loss as a function of range and depth along the azimuths shown in Figure 9 and Figure 10. RAMGeo is a well-tested parabolic equation model suitable for range-dependent fluid seabeds written by Michael Collins from the US Naval Research laboratory. These calculations were performed at one-third octave spaced frequencies from 20 Hz to 1 kHz. Modelling was carried out to a maximum range of 30 km.

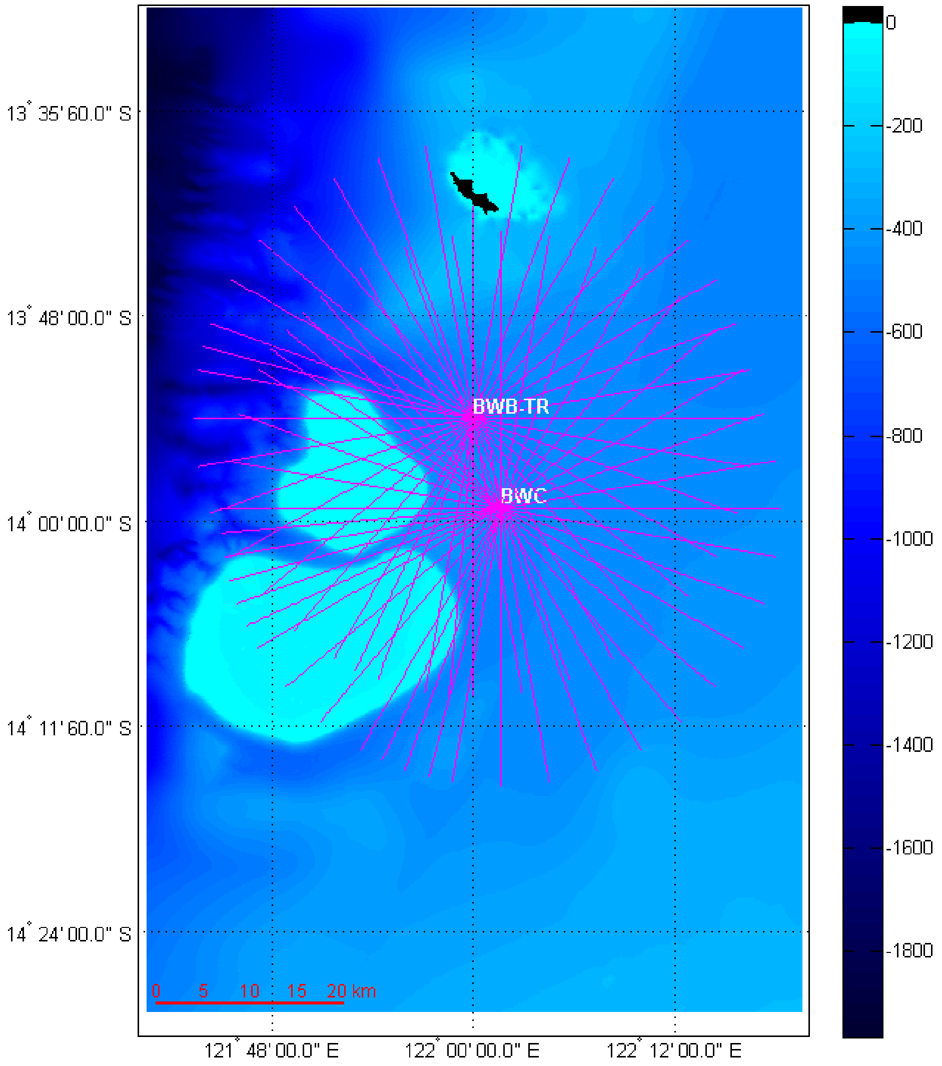

Figure 9. Torosa: Tracks used for acoustic propagation model runs (magenta lines).

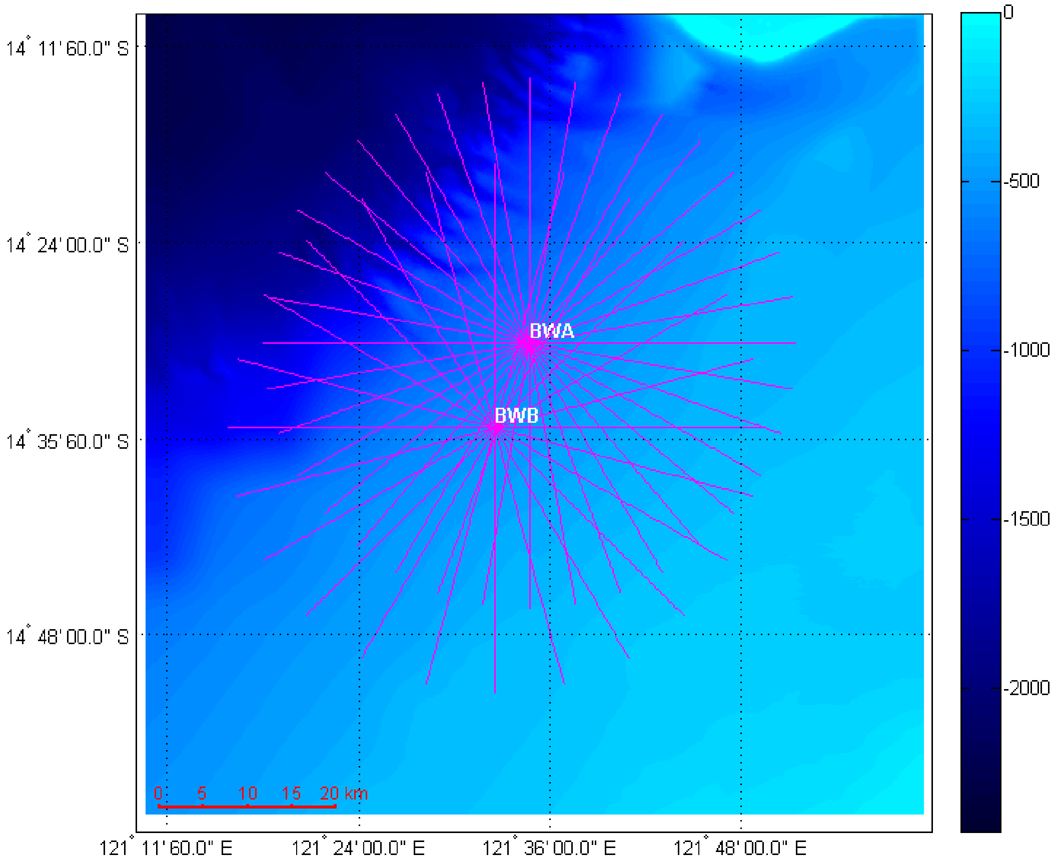

Figure 10. Brecknock/Calliance: Tracks used for acoustic propagation model runs (magenta lines).

Different source depths for the different noise sources made it necessary to carry out three sets of transmission loss calculations, one for each of the source depths shown in Table 6.

For each azimuth, received spectra were calculated as a function of range and depth by subtracting the appropriate transmission loss from the source spectra shown in Figure 5 and Figure 6. The received spectra were then integrated over frequency (in the pressure squared domain), and converted to dB to obtain the received level in dB re 1 µPa root mean square.

Table 6. Modelled source depths

Source type	**Source depth (m)**
Mean and Maximum operational noise	10m
FLNG facility thruster noise	19.5m
Tug thruster noise	7m

The noise produced during LNG carrier berthing includes contributions from the tug thrusters, FLNG facility thrusters and FLNG facility operational noise. This was calculated by modelling the received levels produced by each source individually and then summing the resulting mean squared pressures.

2.5 Modelled scenarios

A number of different scenarios were modelled involving various combinations of operational states of the two FLNGs in each field. In addition to the requested scenarios, which are listed in Table 7.

Table 7. List of modelling scenarios

Scen-ario	Locat-ion	# Facil-ities	Loading / Berthing	Considerations	FLNG mechanical noise	FLNG thruster noise	Tug noise
1	Torosa	1	No	Baseline noise from normal operations.	Mean	-	-
1a	Torosa	1	No	Max noise from normal operations	Max	-	-
2	Torosa	2	No	Baseline noise from normal operations.	Mean	-	-
2a	Torosa	2	No	Max noise from normal operations	Max	-	-
3	Torosa	2	Yes	Berthing of single LNG carrier for offtake at one facility with second facility in normal operation.	BWC-Mean BWB-TR Mean	BWC only	BWC only
3a	Torosa	2	Yes	Berthing of single LNG carrier for offtake at one facility with second facility in normal operation.	BWC-Max BWB-TR Max	BWC only	BWC only
4	Torosa	2	Yes	Dual berthing of LNG carriers alongside both FLNG facilities	BWC-Mean BWB-TR Mean	BWC and BWB-TR	BWC and BWB-TR
4a	Torosa	2	Yes	Dual berthing of LNG carriers alongside both FLNG facilities	BWC-Max BWB-TR Max	BWC and BWB-TR	BWC and BWB-TR
5	Brecknock / Calliance	1	No	Baseline noise from normal operations.	Mean	-	-
5a	Brecknock / Calliance	1	No	Max noise from normal operations	Max	-	-
6	Brecknock / Calliance	2	No	Baseline noise from normal operations.	Mean	-	-
6a	Brecknock / Calliance	2	No	Max noise from normal operations	Max	-	-
7	Brecknock / Calliance	2	Yes	Dual berthing of LNG carriers alongside both FLNG facilities.	BWA-Mean BWB-Mean	BWA and BWB	BWA and BWB
7a	Brecknock / Calliance	2	Yes	Dual berthing of LNG carriers alongside both FLNG facilities.	BWA-Max BWB-Max	BWA and BWB	BWA and BWB

3 Results

3.1 Torosa

Figure 11 plots maps of the maximum predicted received level at any depth for a single FLNG facility operating at BWC and a zoomed version is shown in Figure 12. Each figure presents two plots, one based on FLNG operational noise obtained from the mean measured FPSO operational noise spectrum using the procedure described in Section 2.1, and the other obtained from the maximum measured FPSO operational noise spectrum. There is a difference of approximately 10 dB between the source levels corresponding to these two spectra so it is not surprising that there is a similar difference between the predicted received levels.

These and subsequent sound field plots use a colour scale with a maximum corresponding to 160 dB re 1 µPa because, as can be seen in Figure 12, the facility noise levels rapidly drop below this level (within approximately 100m).

As is expected from theoretical considerations, levels are higher downslope from the source and lower upslope. This is particularly apparent to the north of the source where the seabed rises towards Seringapatam Reef.

Sound can be seen to penetrate the South Reef lagoon along some azimuths. This is made possible by the approximately 40m deep sill along the northern boundary of this lagoon. The low sound levels in the lagoon, and their subsequent rapid reduction with range are an expected result of acoustic propagation up the steep reef slope. Sound is unable to penetrate into the North Reef lagoon because the reef surrounding this lagoon has very little water over it.

Plots of the maximum received level at any depth as a function of range from this single facility are given in Figure 13. This figure includes plots for mean and maximum operational noise and for offloading noise based on both mean and maximum operational noise. The additional thruster cavitation noise present during offloading operations substantially increases the received noise levels above the mean FLNG mechanical noise but only marginally increases it above the maximum FLNG mechanical noise.

The increased scatter in the results at ranges beyond 10km is due to rapid attenuation of sound travelling up the reef slopes compared to sound travelling over flat bathymetry or downslope.

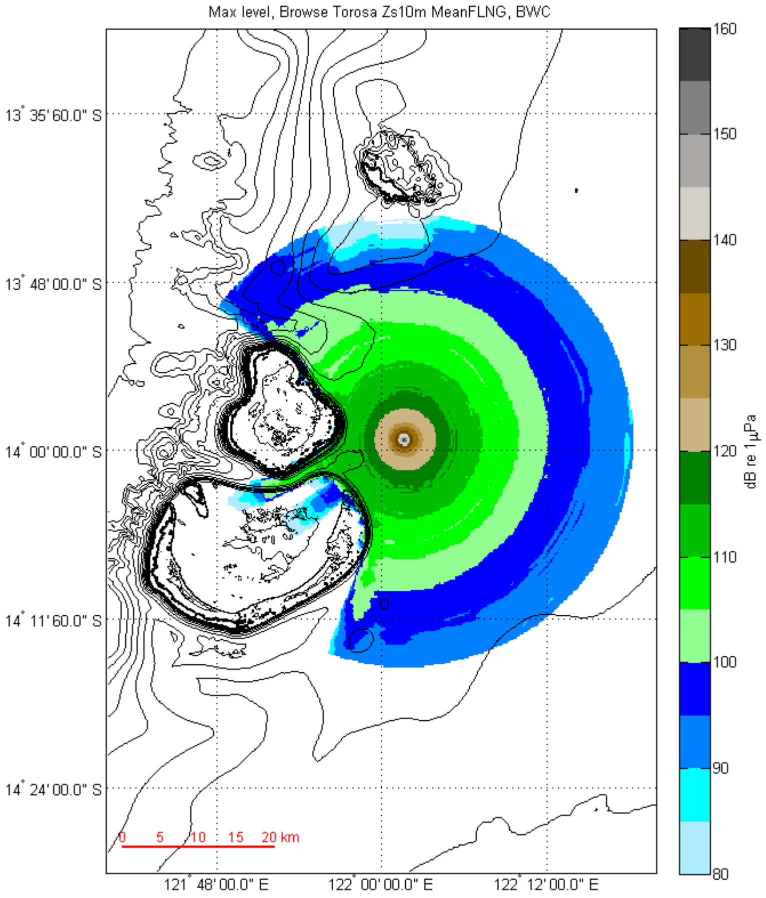

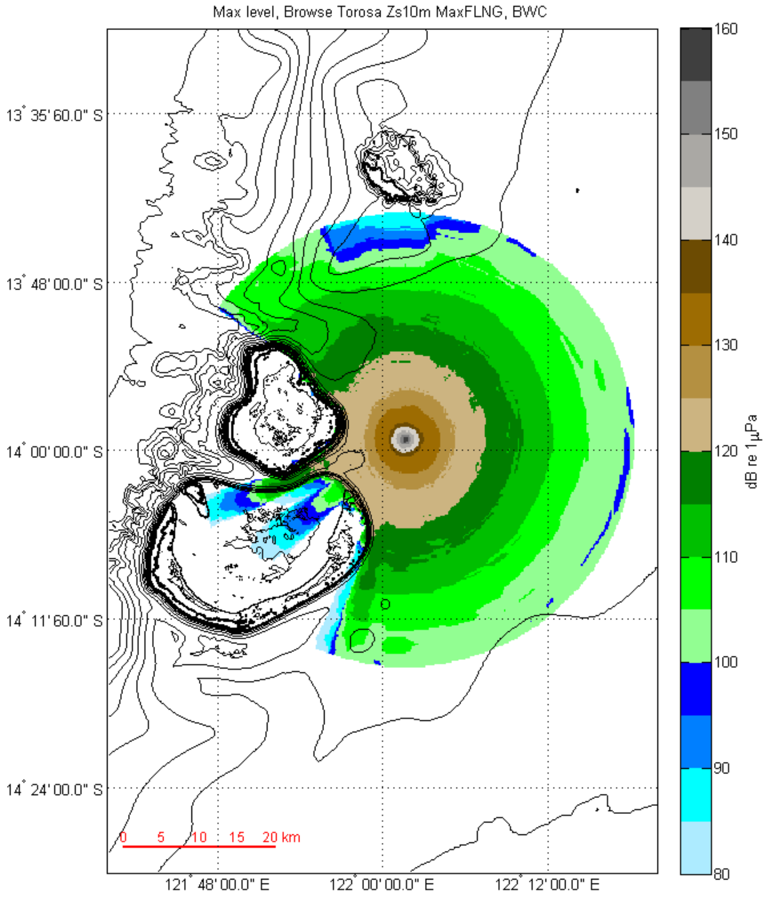

Figure 11. Scenario 1. Maximum received sound pressure level at any depth as a function of geographical position for a single FLNG facility at BWC. Left, mean operational noise. Right, maximum operational noise.

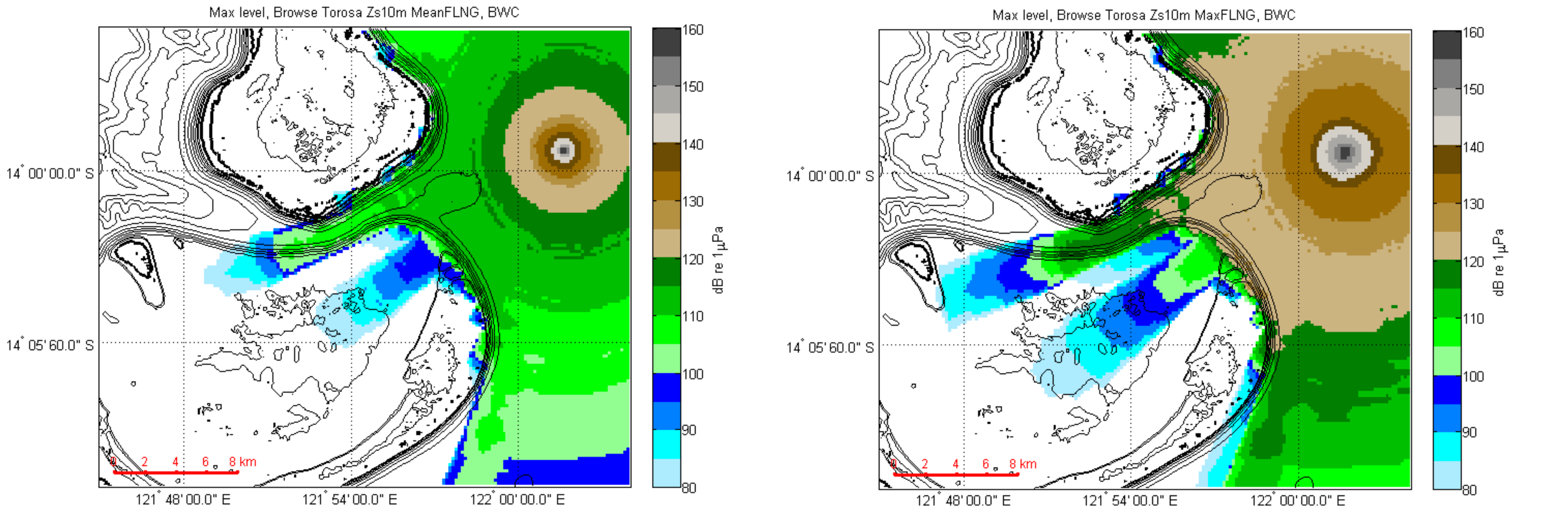

Figure 12. Scenario 1 - zoomed. Maximum received sound pressure level at any depth as a function of geographical position for a single FLNG facility at BWC. Left, mean operational noise. Right, maximum operational noise.

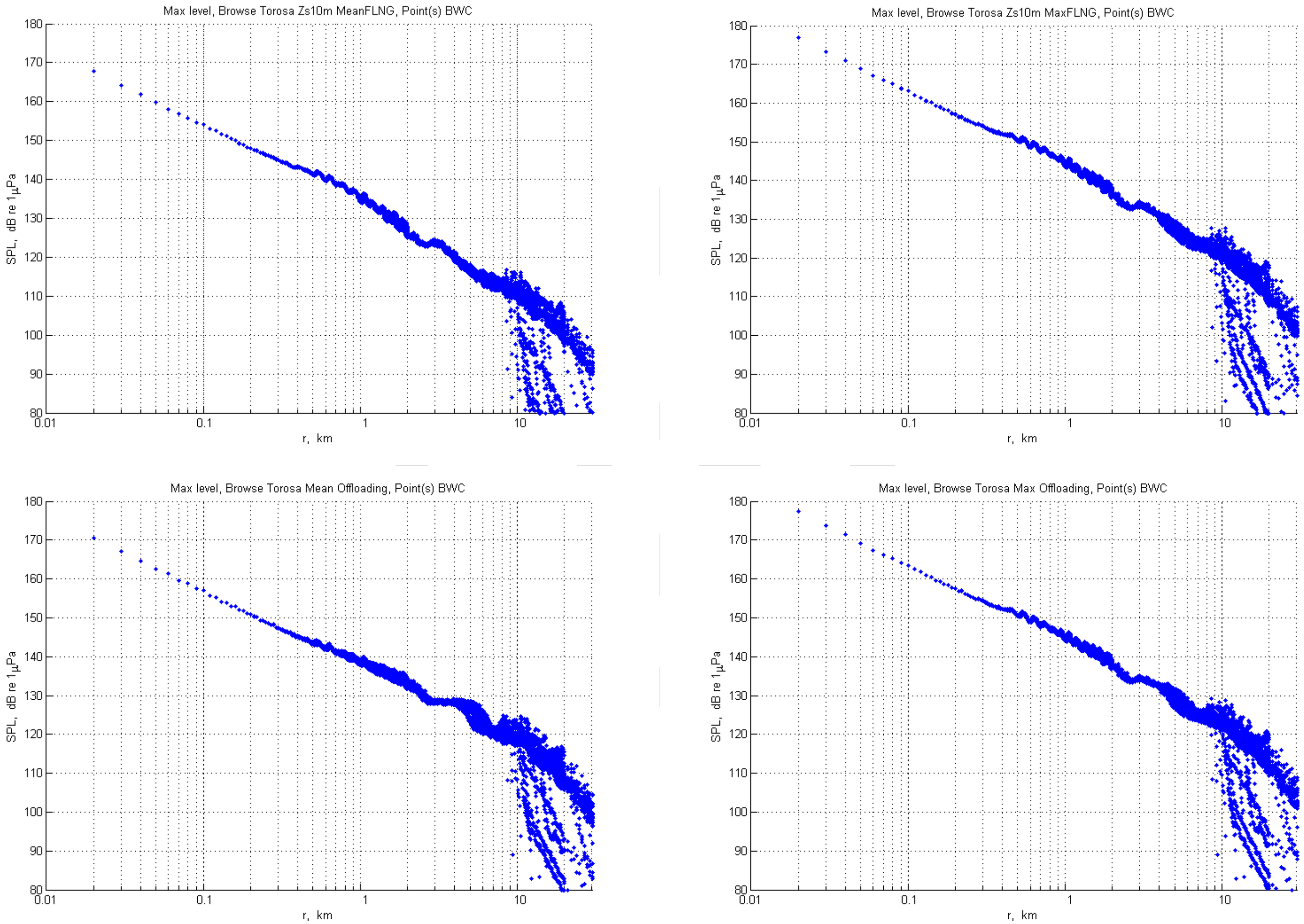

Figure 13. Scenario 1. Scatter plots of maximum received level versus range for all azimuths from a single facility at BWC. Top left is mean operational noise, top right is maximum operational noise, bottom left is offloading noise based on mean operational noise, bottom right is offloading noise based on maximum operational noise.

Figure 15 compares the maximum received level at any depth as a function of range from BWC along the azimuth that penetrates furthest into the channel between North and South Scott Reef (shown in Figure 14) for mean operational noise, maximum operational noise, offloading noise based on mean operational noise and offloading noise based on maximum operational noise. The sound attenuates rapidly beyond 20km as it propagates up the reef slope and into the reef lagoon. Again it can be seen that the offloading results in only a slight increase in received levels over the maximum operational noise.

Figure 16 shows vertical cross-sections of the sound field along this azimuth, the location of which is shown in Figure 14.

Maps of the maximum received level at any depth for scenarios 2, 3, and 4 are given in Figure 17 through to Figure 22. Sound levels from multiple sources add energetically, and a doubling of energy corresponds to an increase in sound pressure level of 3 dB. When two sources are operating, and there is a difference of more than a few dB between the received levels that each produces at a given location, then the combined received level at that location will be determined by the loudest source. If both sources produce similar sound levels, then the combined received level will be up to 3 dB higher than the received level due to an individual source. The results shown in these figures are in agreement with these expectations.

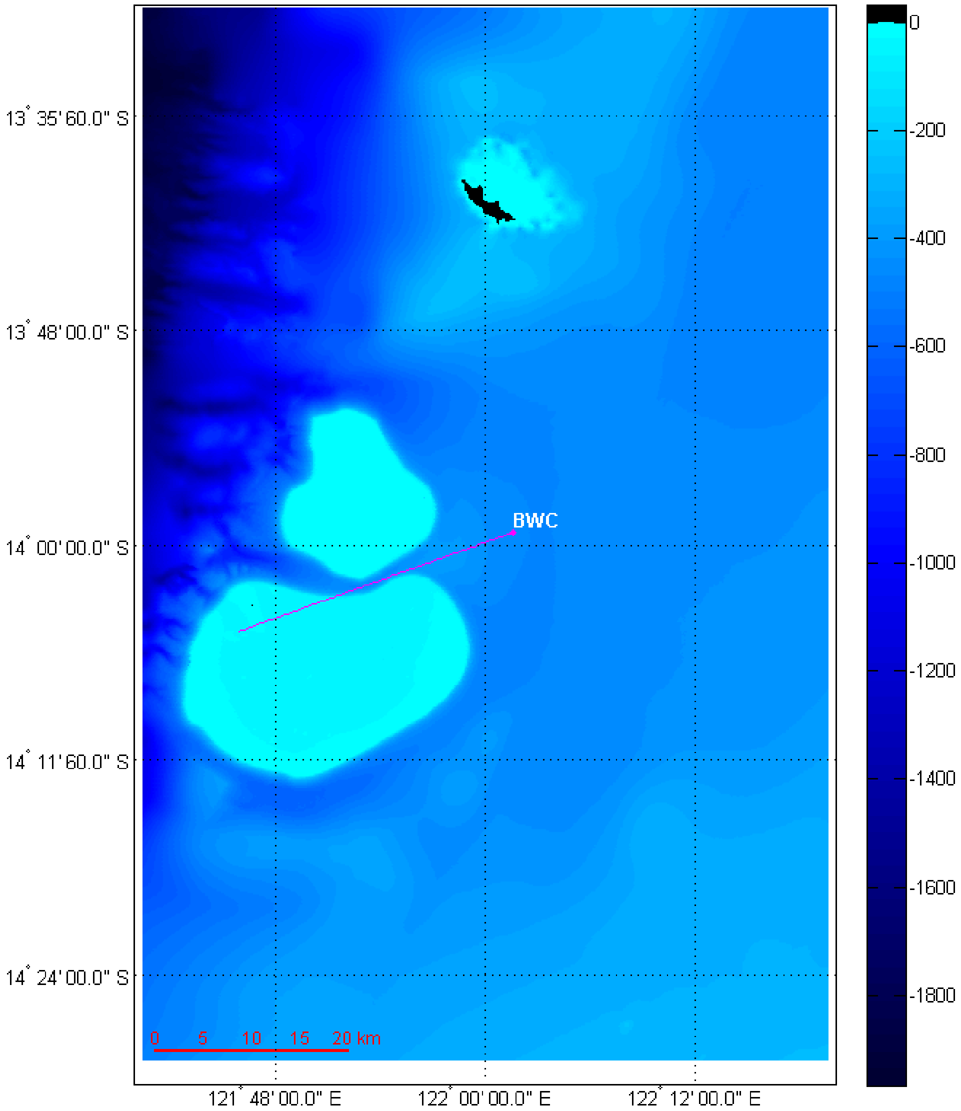

Figure 14. Map showing the azimuth from BWC (250°) that penetrates furthest into the channel between North and South Scott Reef.

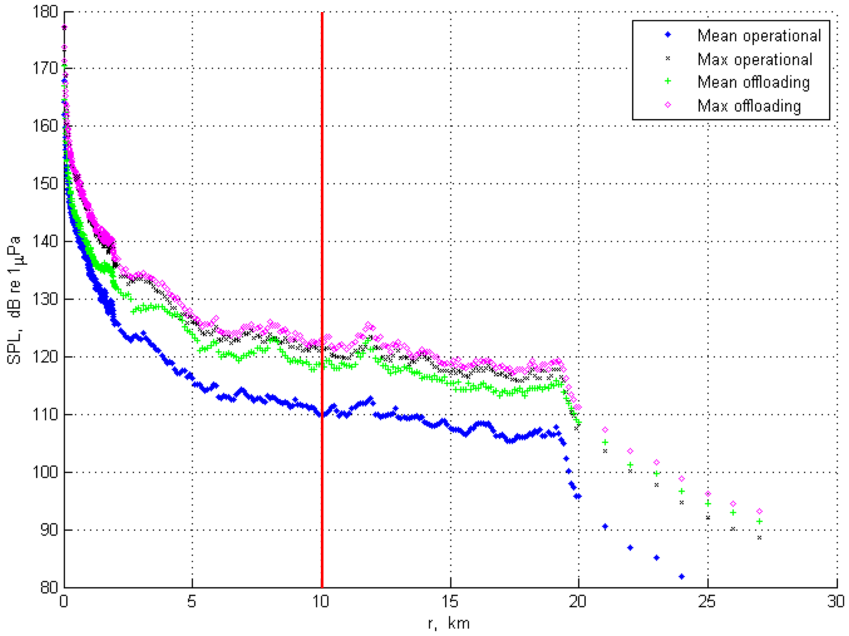

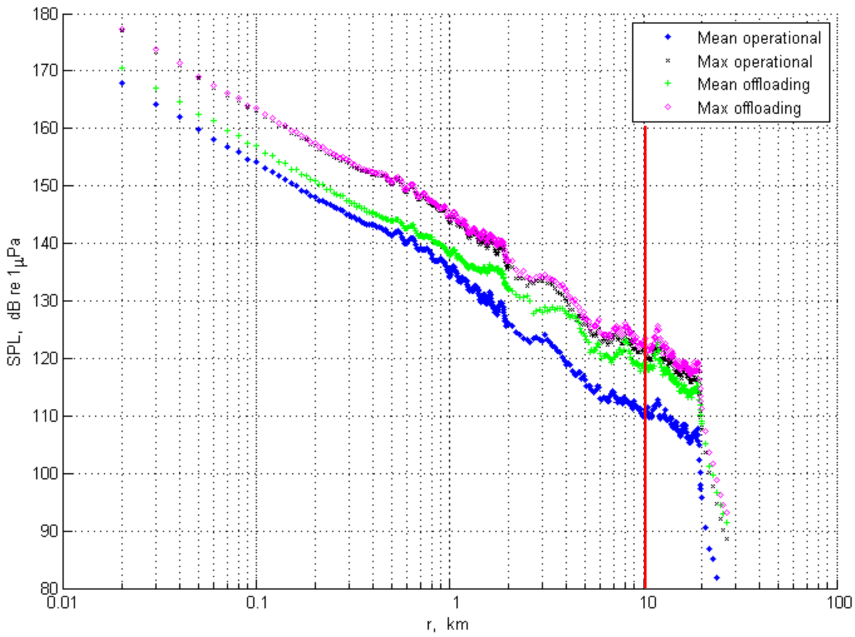

Figure 15. Scenario 1. Plots of the maximum level at any depth as a function of range from the source along 250° azimuth from BWC for mean operational noise, maximum operational noise, offloading noise based on mean operational noise, and offloading noise based on maximum operational noise. Both plots show the same data but are plotted using a linear range scale (top) and a logarithmic range scale (bottom). The vertical red line in each plot marks the nominal entrance to the channel.

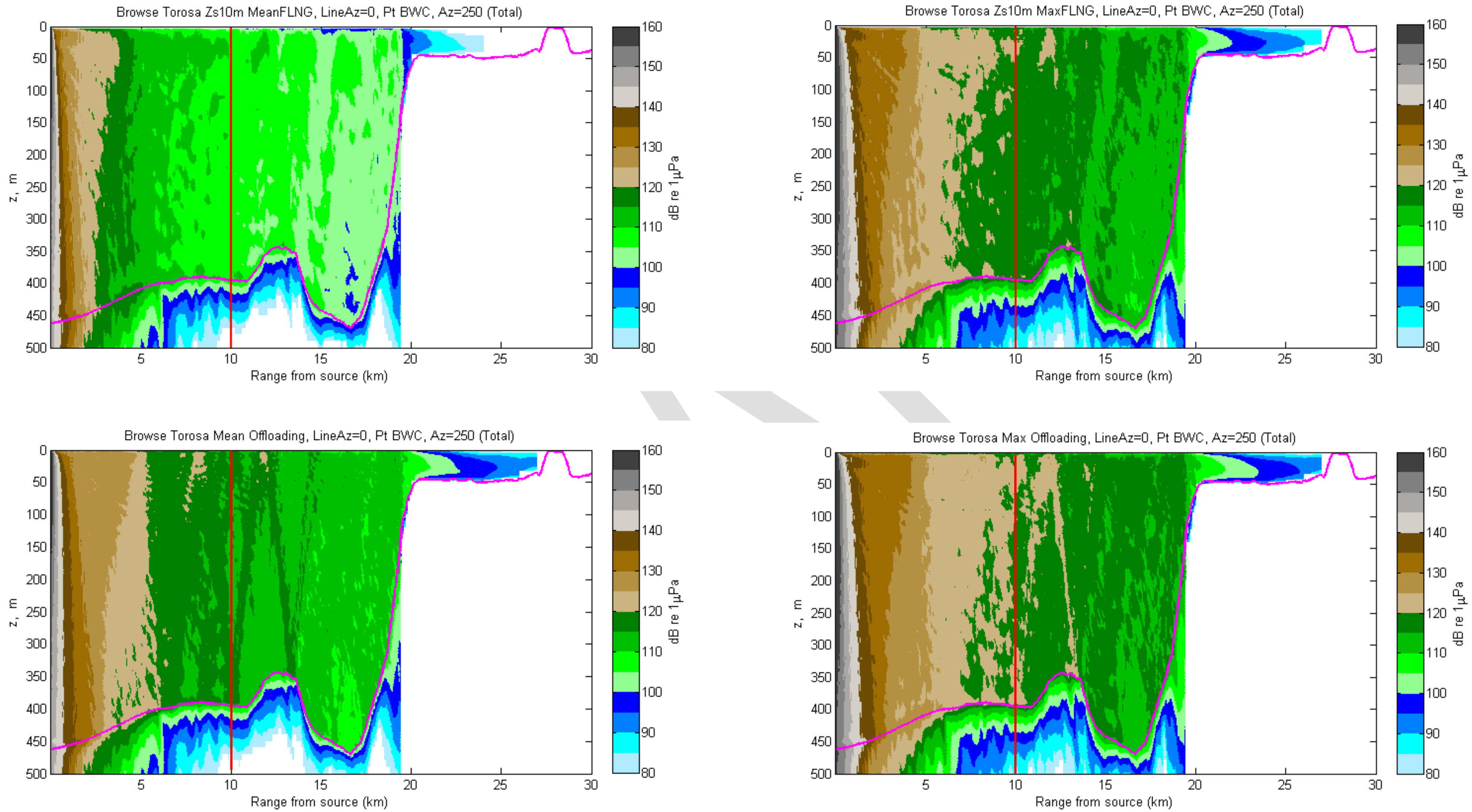

Figure 16. Scenario 1. Vertical cross-sections through the received sound field along the azimuth from BWC (250°) that penetrates furthest into the channel between North and South Scott Reef. Top left is for mean operational noise, top right is for maximum operational noise, bottom left is for offloading noise based on mean operational noise, bottom right is for offloading noise based on maximum operational noise. The vertical red line in each plot marks the nominal entrance to the channel. These results are for a single FLNG facility at BWC.

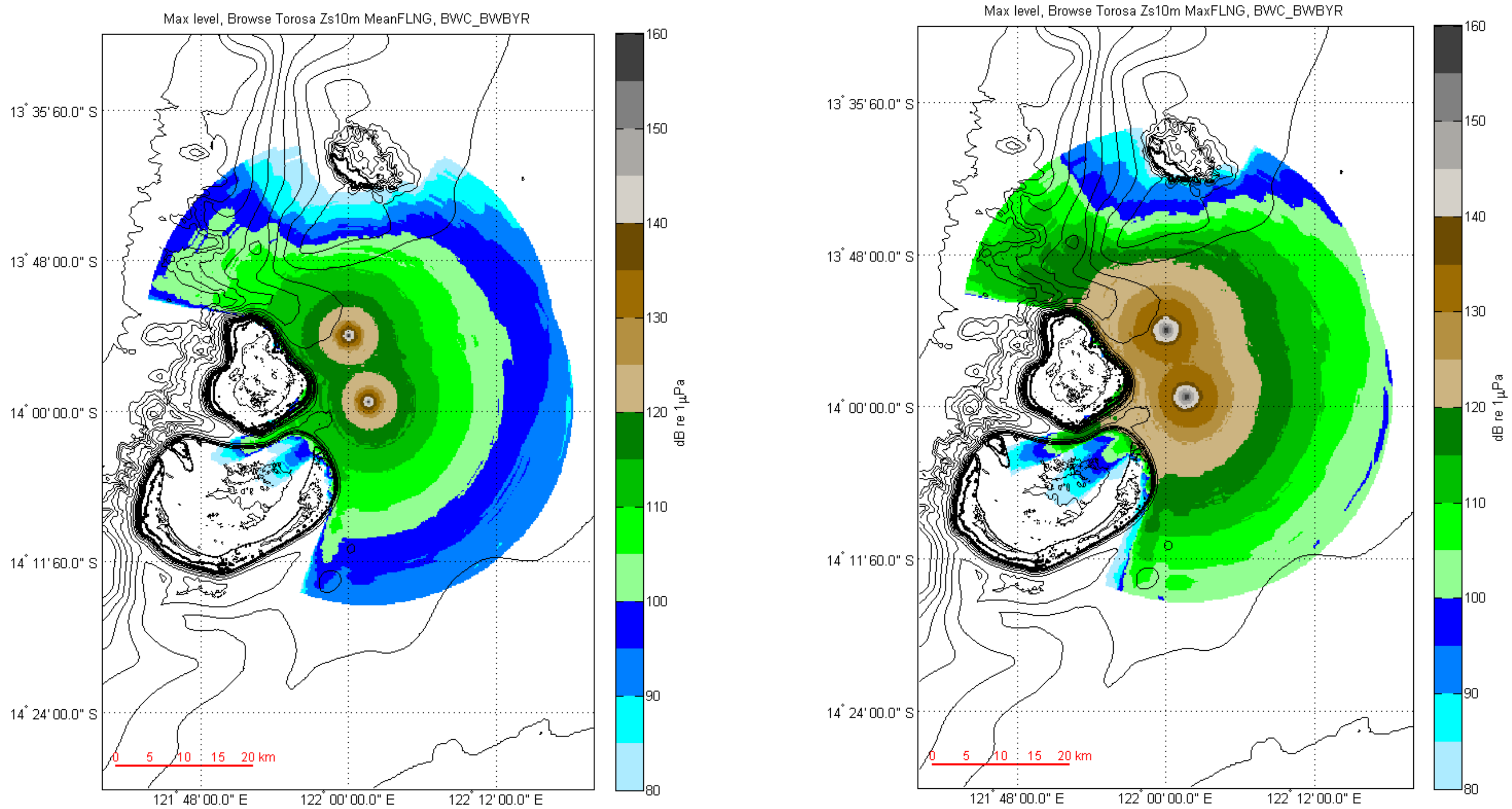

Figure 17. Scenario 2. Maximum received sound pressure level at any depth as a function of geographical position for simultaneously operating FLNG facilities at BWC and BWB-TR. Left, mean operational noise at both facilities. Right, maximum operational noise at both facilities.

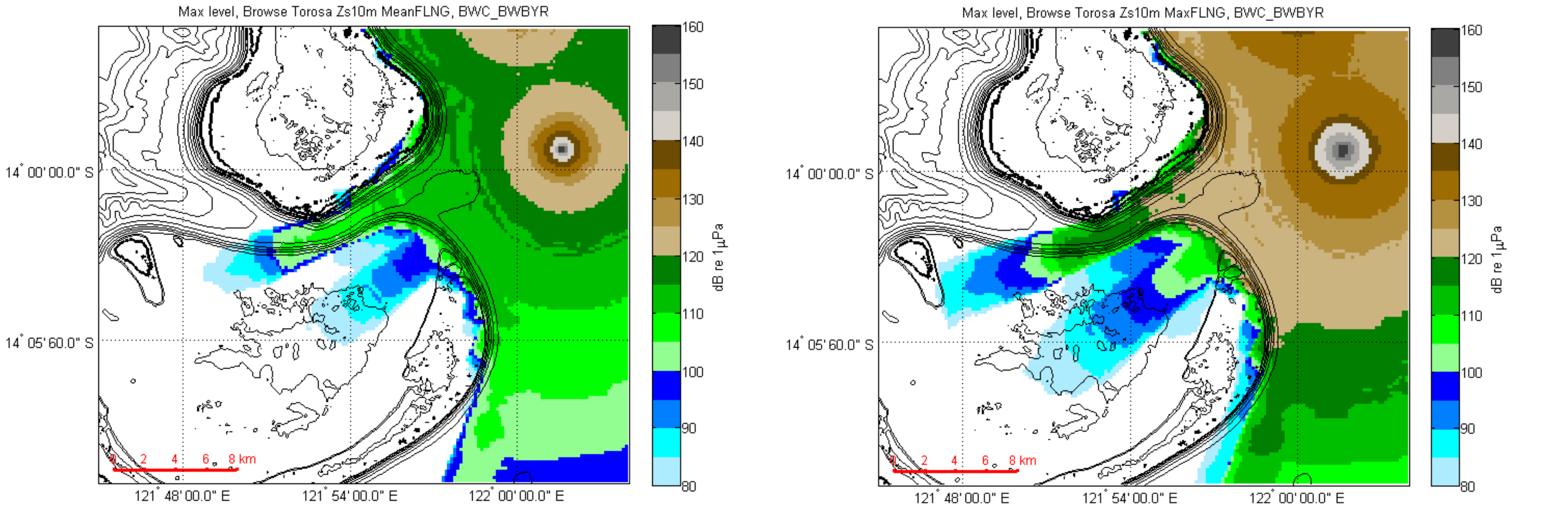

Figure 18. Scenario 2 - zoomed. Maximum received sound pressure level at any depth as a function of geographical position for simultaneously operating FLNG facilities at BWC and BWB-TR. Left, mean operational noise at both facilities. Right, maximum operational noise at both facilities.

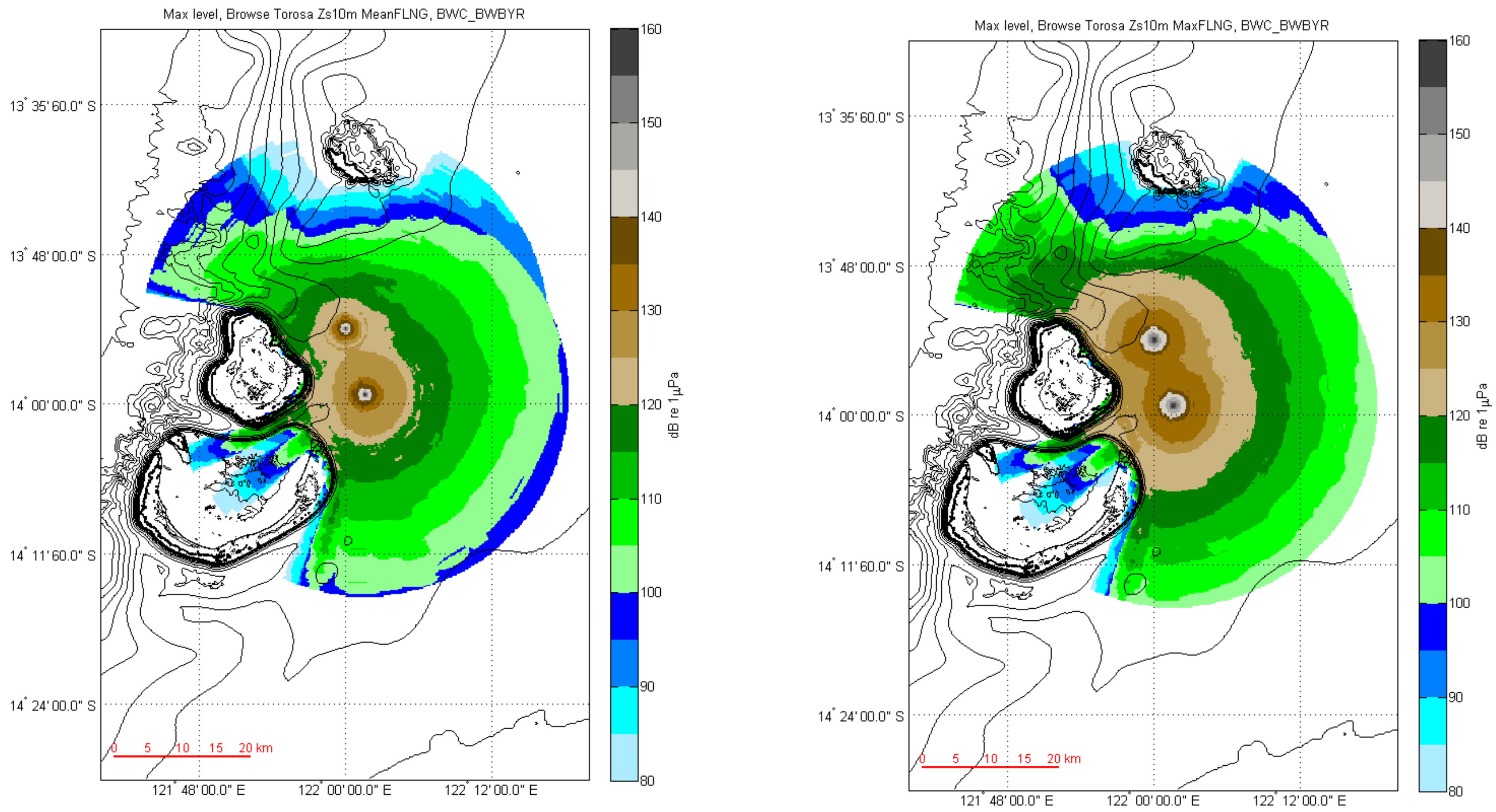

Figure 19. Scenario 3. Maximum received sound pressure level at any depth as a function of geographical position for an FLNG offloading at BWC while a second FLNG is carrying out normal operations at BWB-TR. Left, calculations based on mean operational noise at both facilities. Right, calculations based on maximum operational noise at both facilities. (See text for more explanation.)

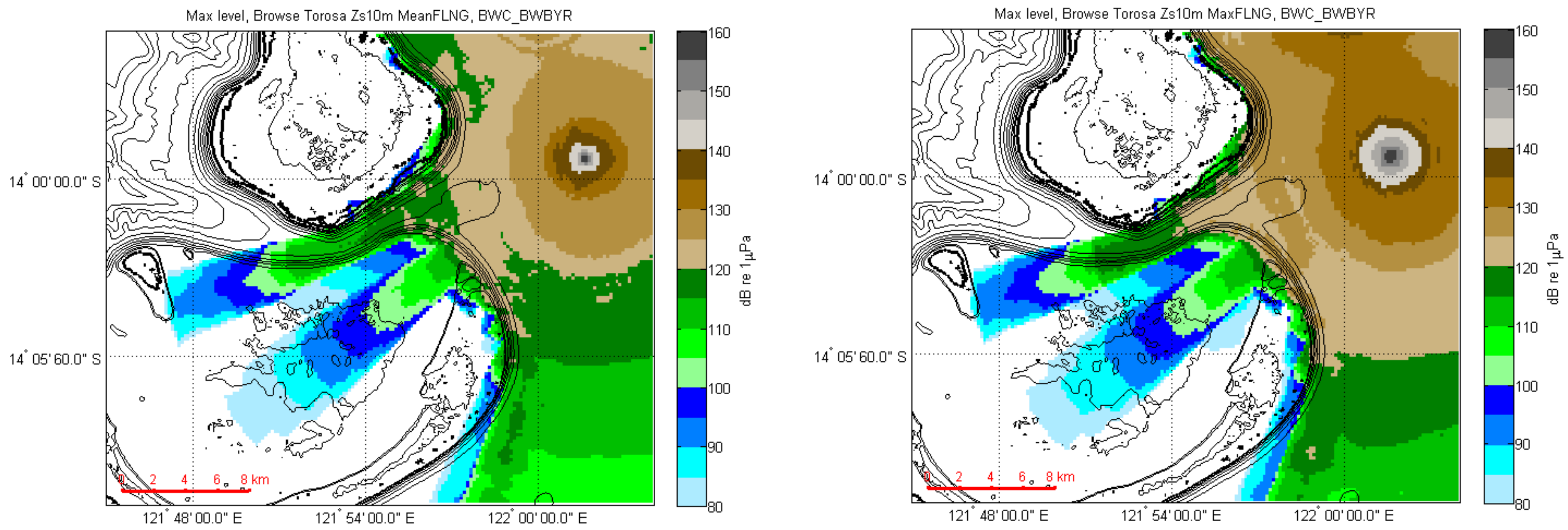

Figure 20. Scenario 3 - zoomed. Maximum received sound pressure level at any depth as a function of geographical position for an FLNG offloading at BWC while a second FLNG is carrying out normal operations at BWB-TR. Left, calculations based on mean operational noise at both facilities. Right, calculations based on maximum operational noise at both facilities. (See text for more explanation.)

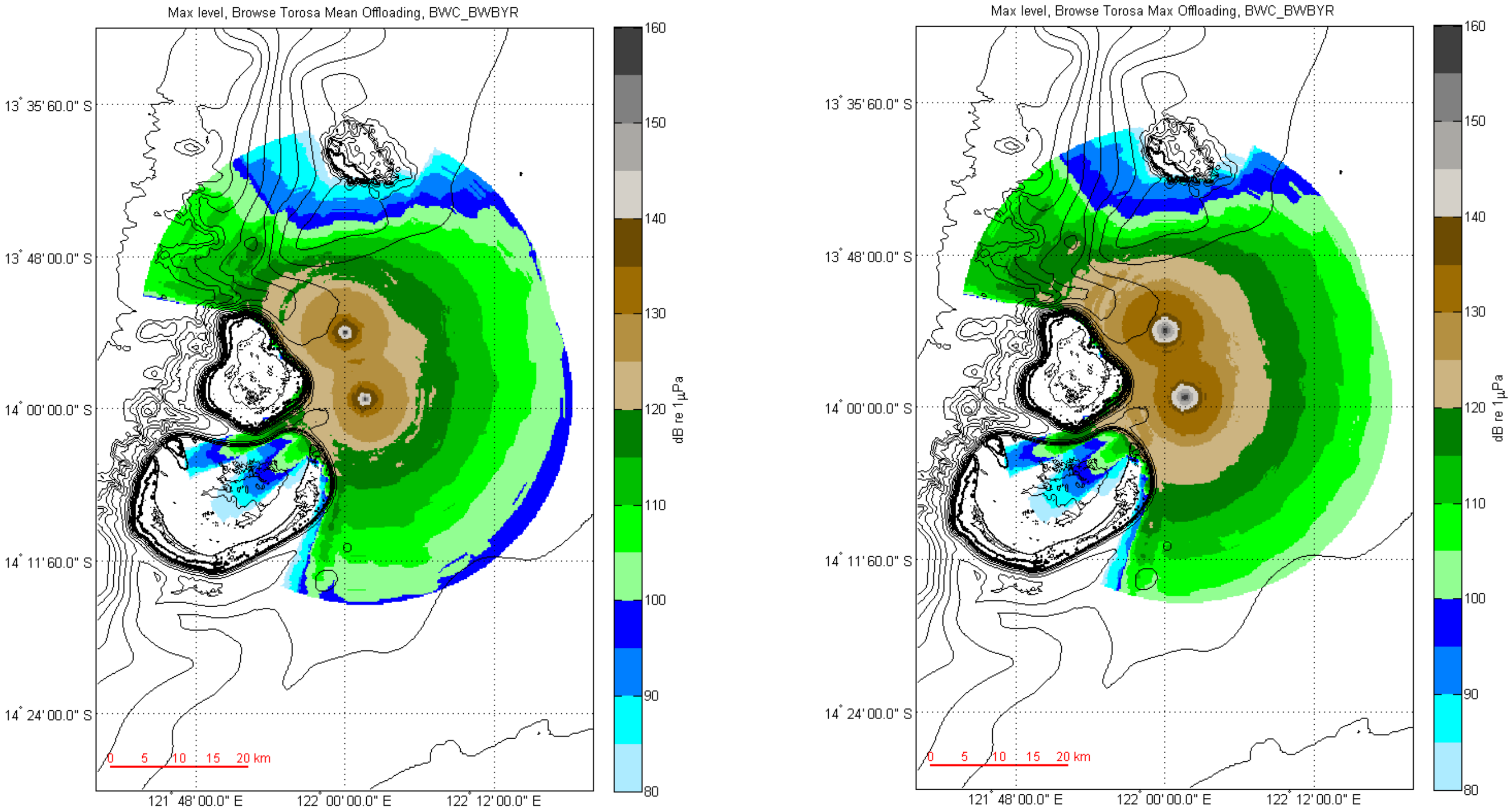

Figure 21. Scenario 4. Maximum received sound pressure level at any depth as a function of geographical position for an FLNG offloading at BWC while a second FLNG carries out offloading operations at BWB-TR. Left, calculations based on mean operational noise at both facilities. Right, calculations based on maximum operational noise at both facilities. (See text for more explanation.)

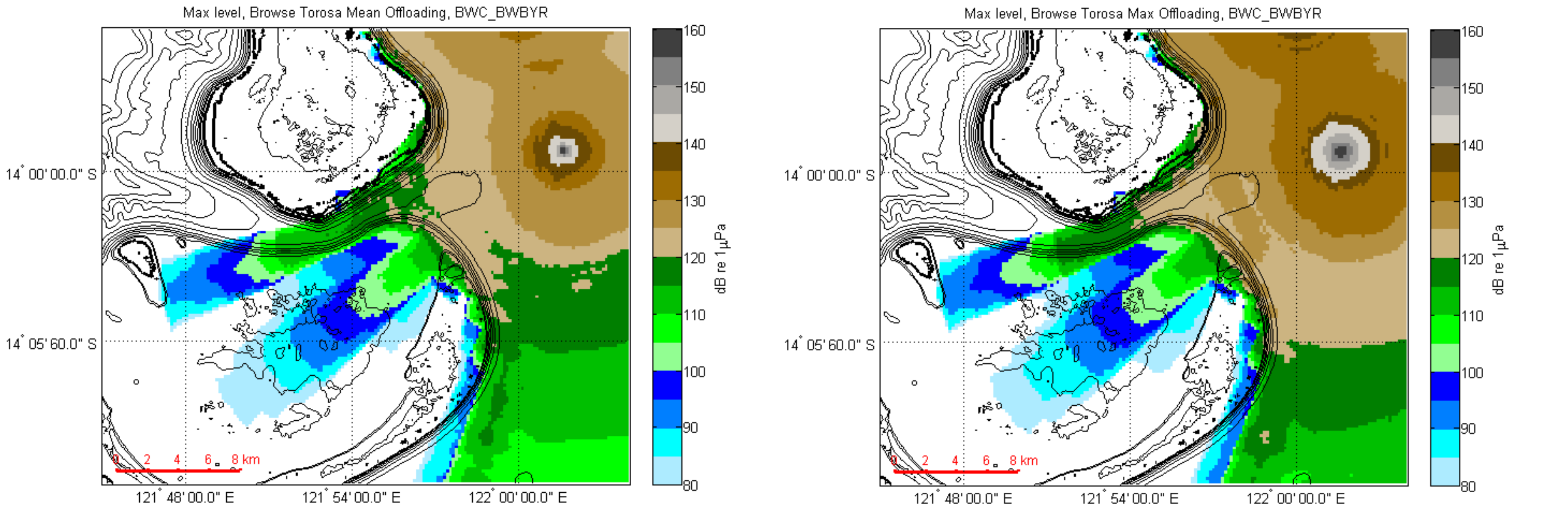

Figure 22. Scenario 4 - zoomed. Maximum received sound pressure level at any depth as a function of geographical position for an FLNG offloading at BWC while a second FLNG carries out offloading operations at BWB-TR. Left, calculations based on mean operational noise at both facilities. Right, calculations based on maximum operational noise at both facilities. (See text for more explanation.)

West-east and south-north vertical cross-sections through the sound field were output for scenarios 1 to 4 and are plotted in Figure 24 through to Figure 27. The locations of these cross-sections are shown in the map given in Figure 23. It should be noted that there is a slight mismatch between the magenta line showing the seabed in these plots and the sound field, which is an artefact of the gridding process and a result of the calculation of the sound field along radials that are relatively coarsely spaced in azimuth.

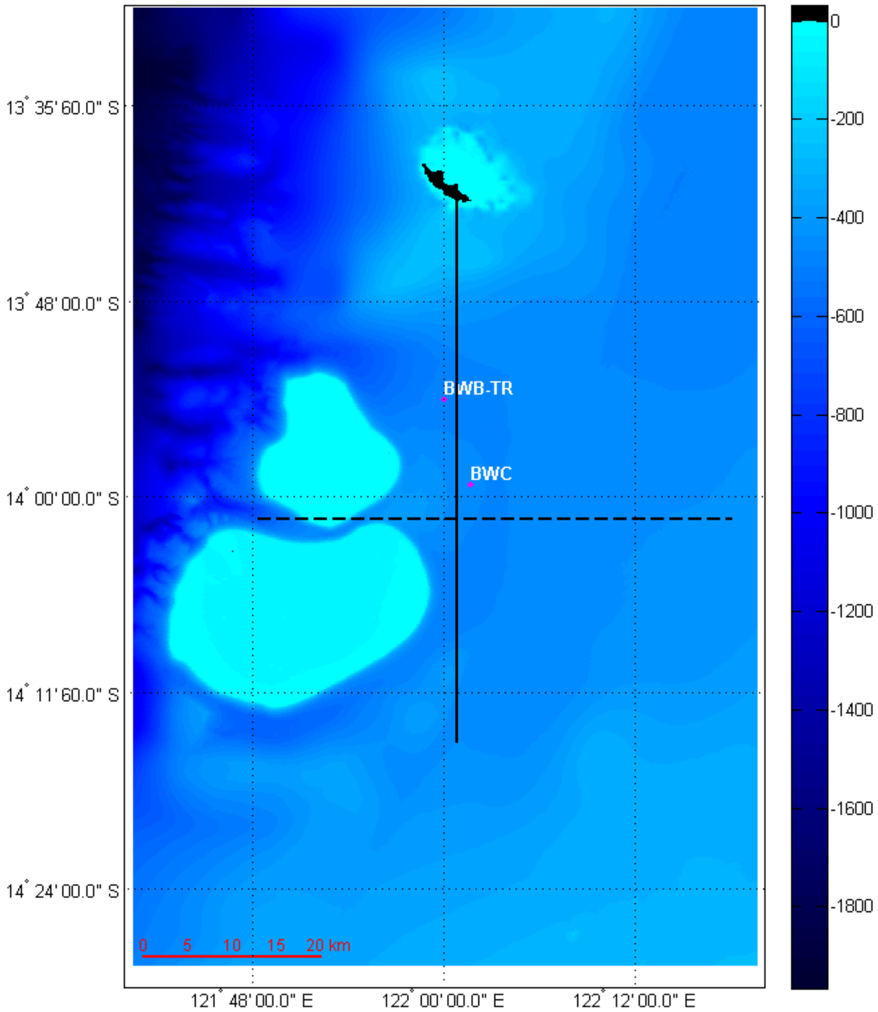

Figure 23. Map showing locations of west-east (broken black line) and south-north (solid black line) cross-sections of the sound field plotted in the following figures.

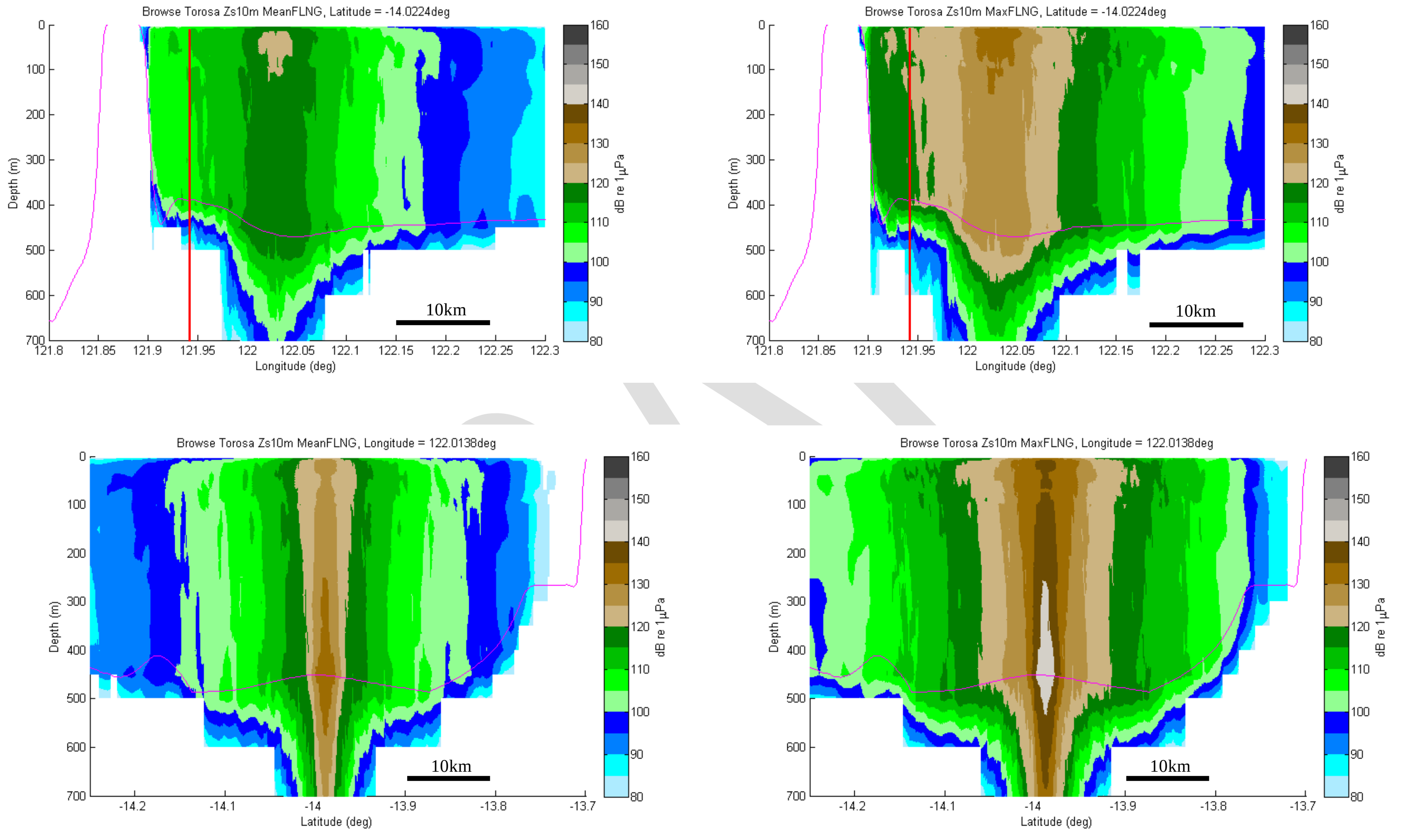

Figure 24. West-East (top) and South-North (bottom) cross sections through the gridded sound field for Scenario 1. Left hand plots are for mean FLNG operational noise, right hand plots are for maximum FLNG operational noise. The vertical red lines in the top two plots mark the longitude of the nominal entrance to the channel.

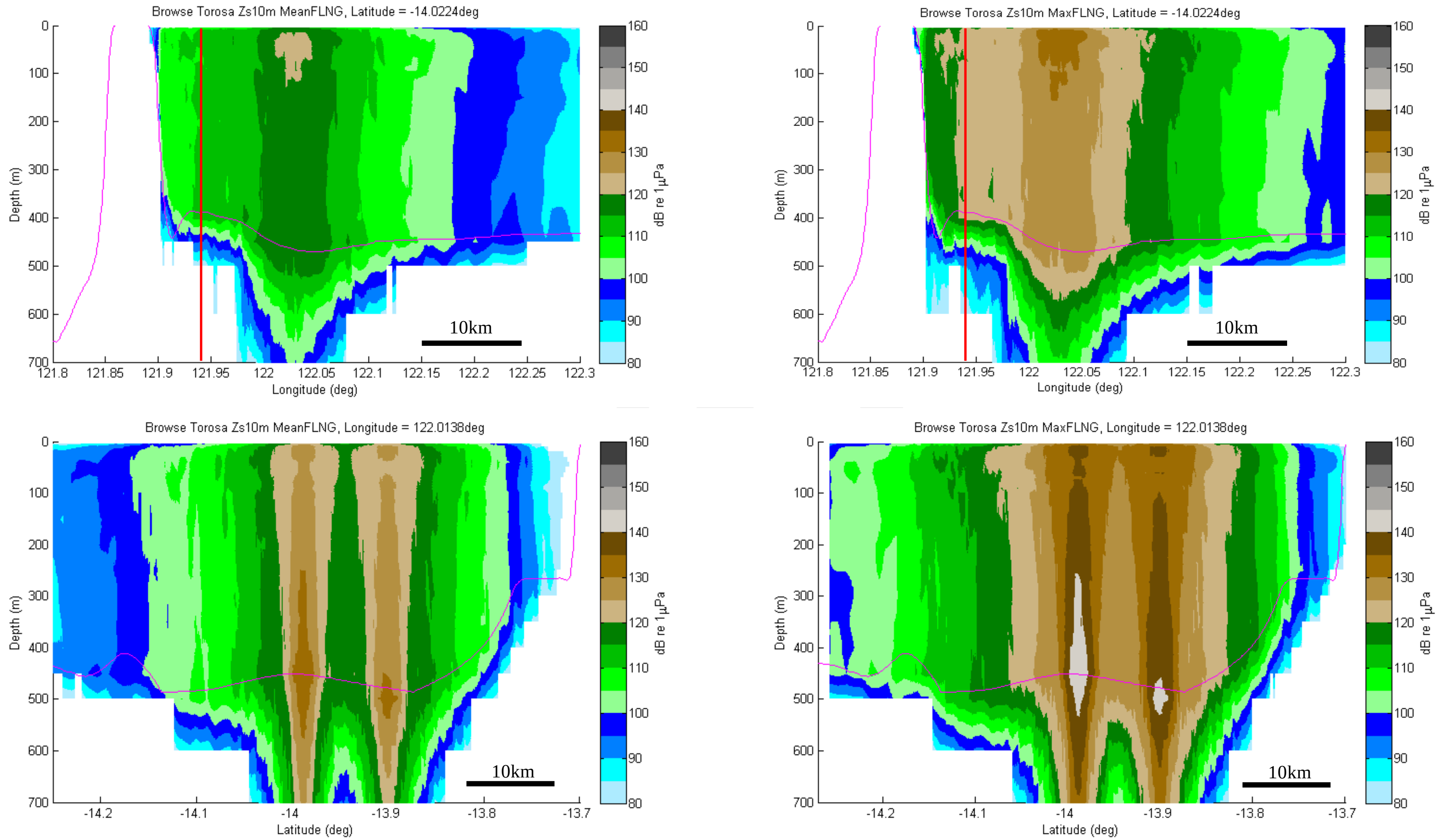

Figure 25. West-East (top) and South-North (bottom) cross sections through the gridded sound field for Scenario 2. Left hand plots are for mean FLNG operational noise, right hand plots are for maximum FLNG operational noise. The vertical red lines in the top two plots mark the longitude of the nominal entrance to the channel.

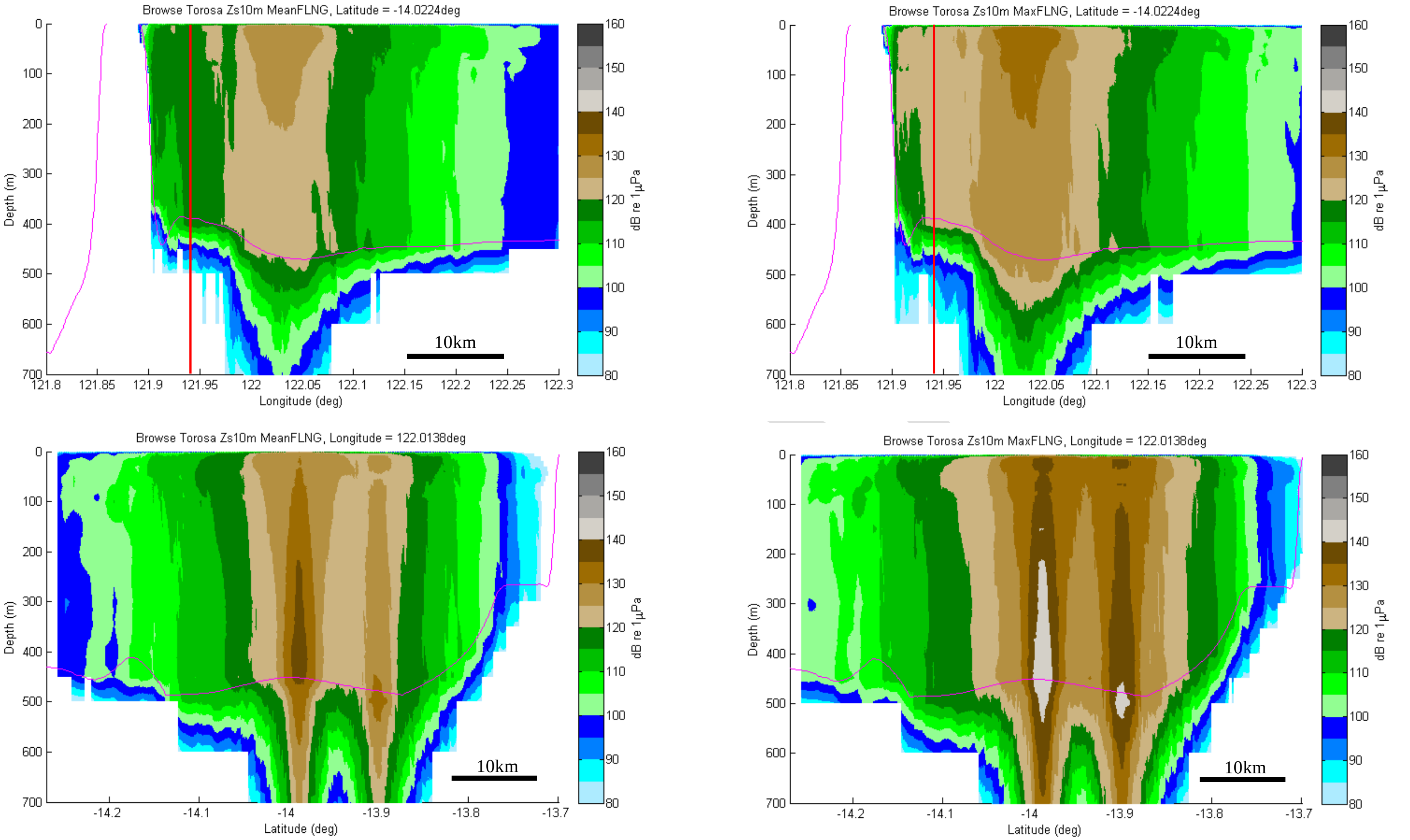

Figure 26. West-East (top) and South-North (bottom) cross sections through the gridded sound field for Scenario 3. Left, calculations based on mean operational noise at both facilities. Right, calculations based on maximum operational noise at both facilities. The vertical red lines in the top two plots mark the longitude of the nominal entrance to the channel.

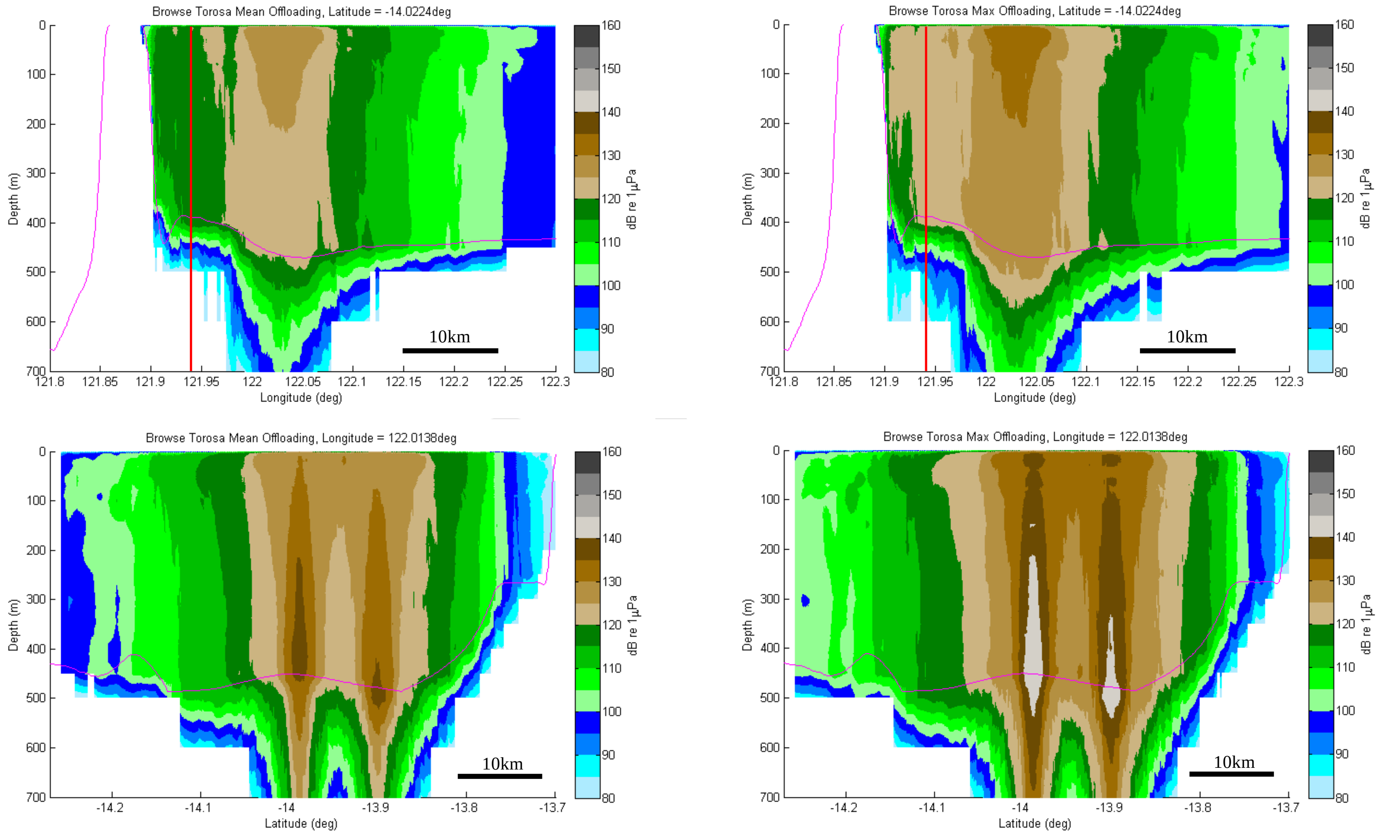

Figure 27. West-East (top) and South-North (bottom) cross sections through the gridded sound field for Scenario 4. Left, calculations based on mean operational noise at both facilities. Right, calculations based on maximum operational noise at both facilities. The vertical red lines in the top two plots mark the longitude of the nominal entrance to the channel.

3.2 Brecknock/Calliance

Plots showing the maximum received sound level at any depth as a function of geographical location for Scenario 5 (a single FLNG facility at BWA) are shown in Figure 28 for both mean and maximum operational noise. Again there is a pronounced asymmetry, with the levels at a given range being highest downslope from the source. This effect is further illustrated in Figure 29 which shows a vertical cross-section through the sound field produced by a single FLNG at BWA for the mean operational noise case. The geographical location of this cross-section is shown in Figure 30.

In the offshore direction the sound is refracted downwards by the sound speed profile and tends to concentrate near the seabed, whereas upslope propagation inshore distributes the sound fairly uniformly throughout the water column.

Scatter plots of the maximum received level at any depth as a function of range from the source are given in Figure 31 for both operational and offloading noise. The peaks visible in these plots at ranges of 6 km and more are a result of localised focussing of sound by a combination of the seabed shape and refraction by the water column sound speed profile.

Figure 32 and Figure 33 show geographical plots of the maximum received level at any depth for scenarios 6 and 7 which are for operational noise (Figure 32, scenario 6) and offloading noise (Figure 33, scenario 7) occurring simultaneously at BWA and BWB.

West-east and south-north cross sections through the sound fields produced by scenarios 6 and 7 are shown in Figure 35 and Figure 36. A map showing the locations of these cross sections is given in Figure 34.

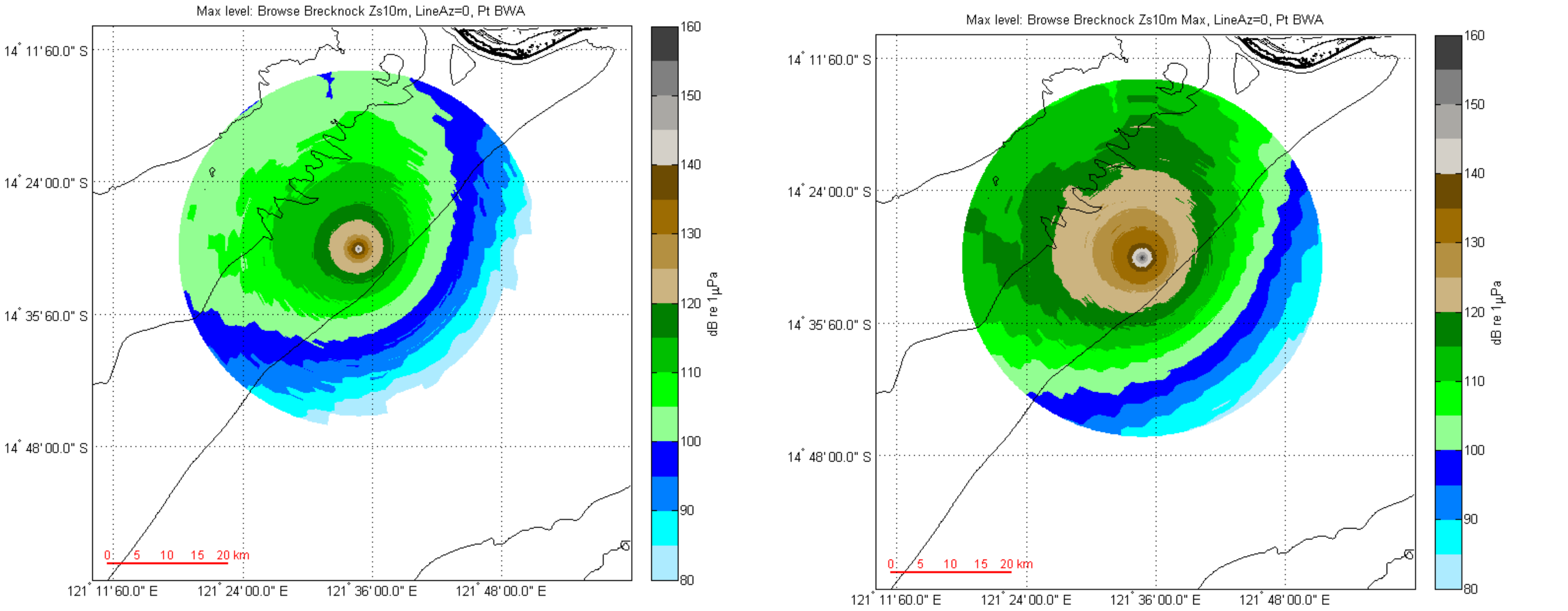

Figure 28 Scenario 5. Maximum received sound pressure level at any depth as a function of geographical position for a single FLNG facility at BWA. Left, mean operational noise. Right, maximum operational noise.

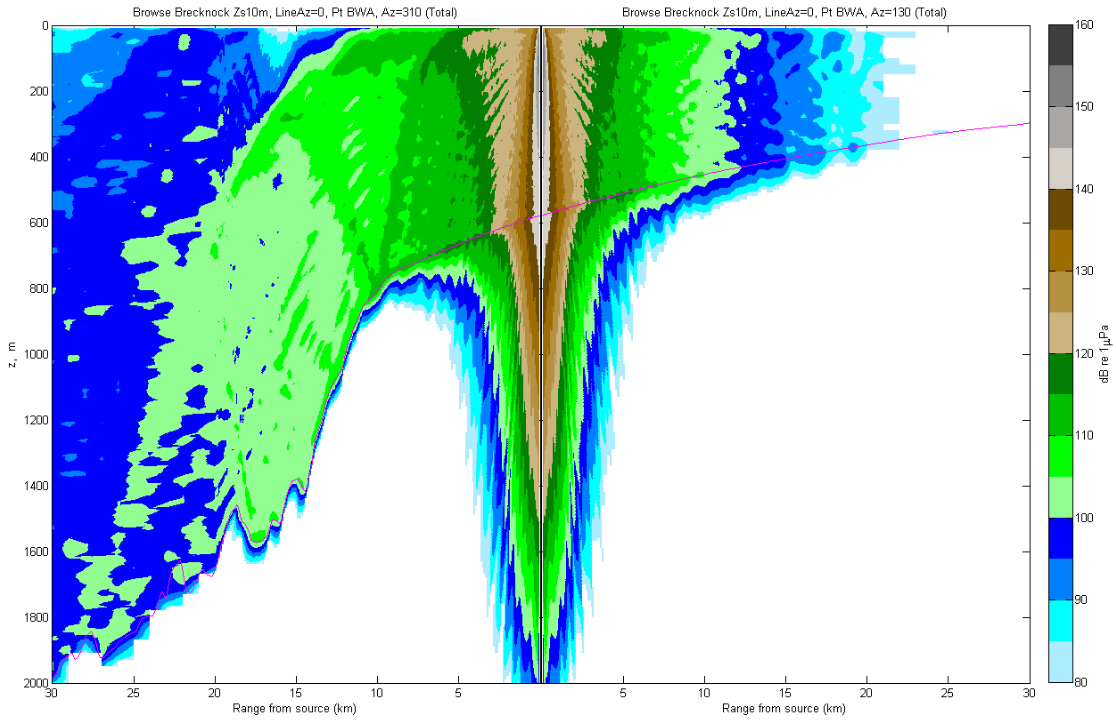

Figure 29. Scenario 5. Cross-section of the sound field produced by a single FLNG at BWA emitting mean operational along the 310° and 130° azimuths shown in Figure 30. The source is at the centre of the plot.

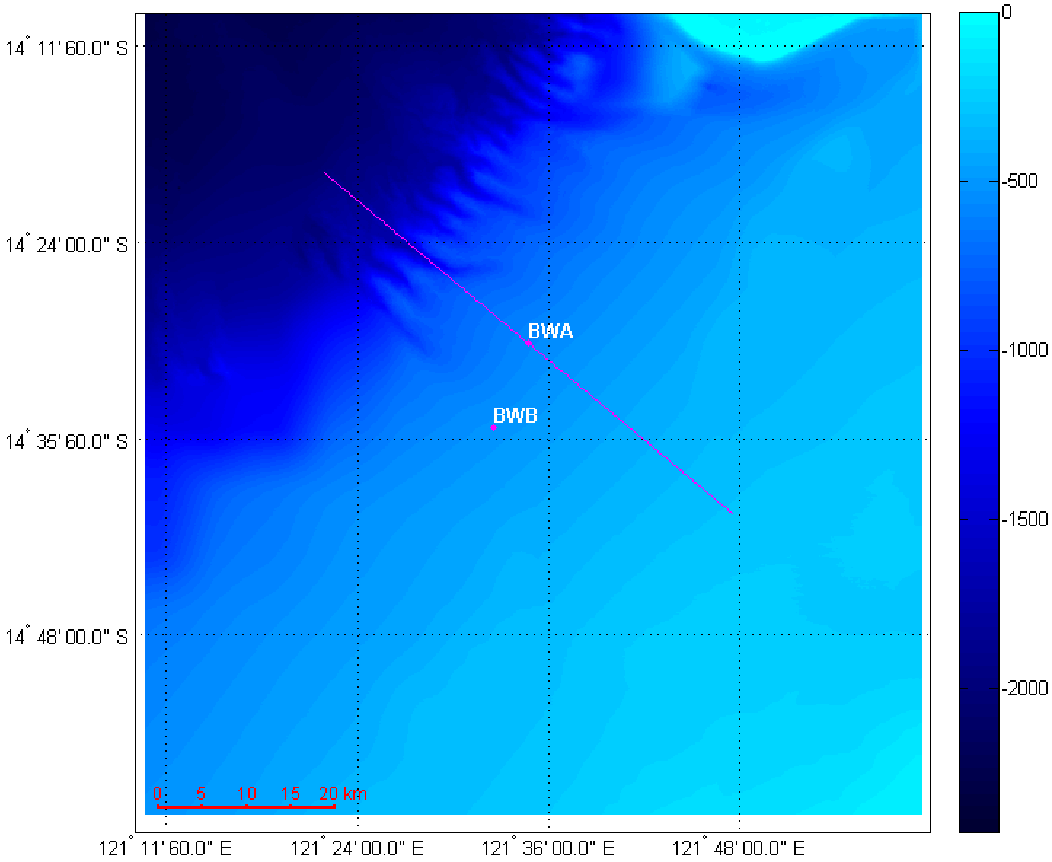

Figure 30. Map showing the 310° and 130° azimuths from BWA that are used for the cross-section plot in Figure 29.

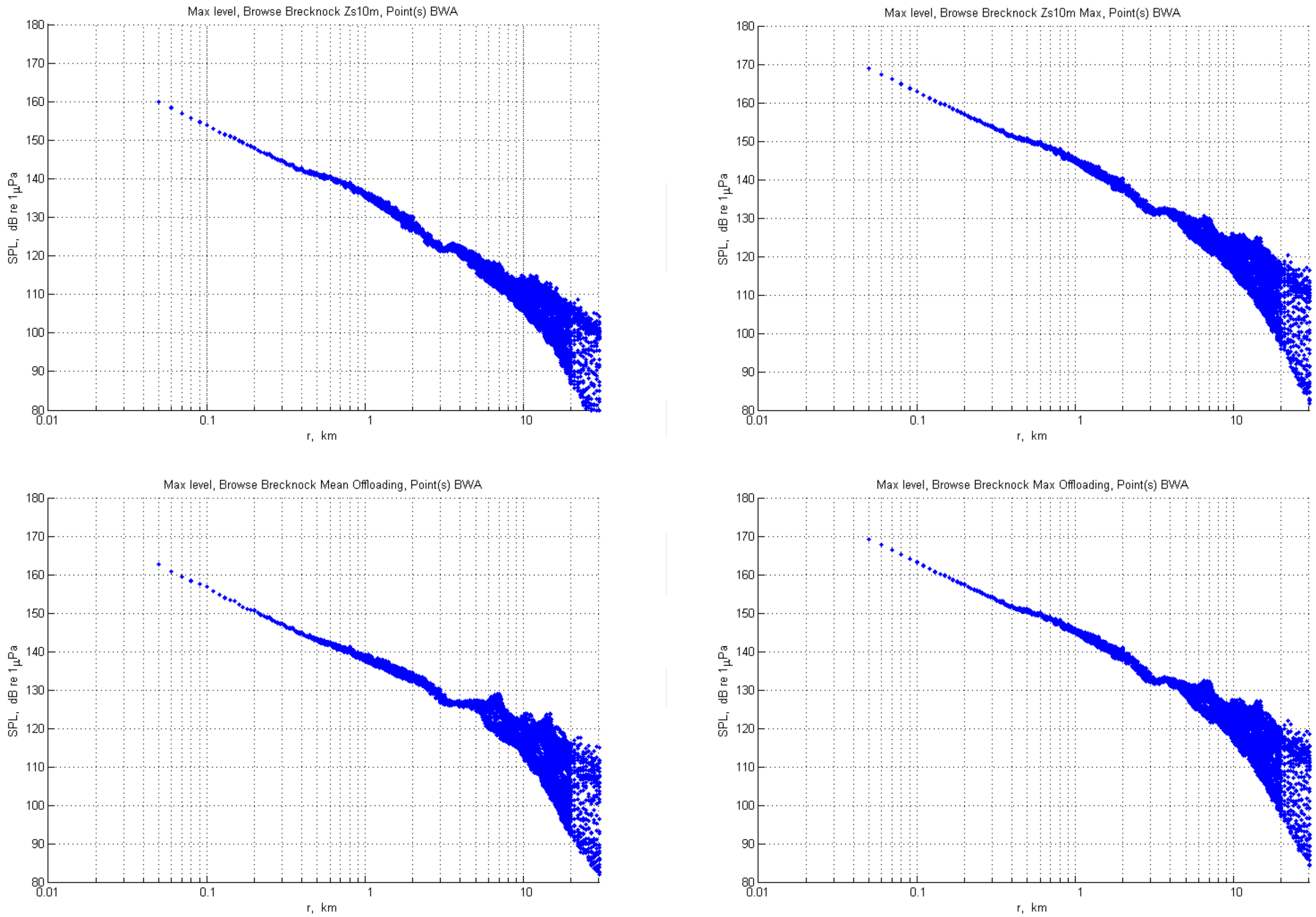

Figure 31. Scenario 5. Scatter plots of maximum received level versus range for all azimuths from a single facility at BWC. Top left is mean operational noise, top right is maximum operational noise, bottom left is offloading noise based on mean operational noise, bottom right is offloading noise based on maximum operational noise

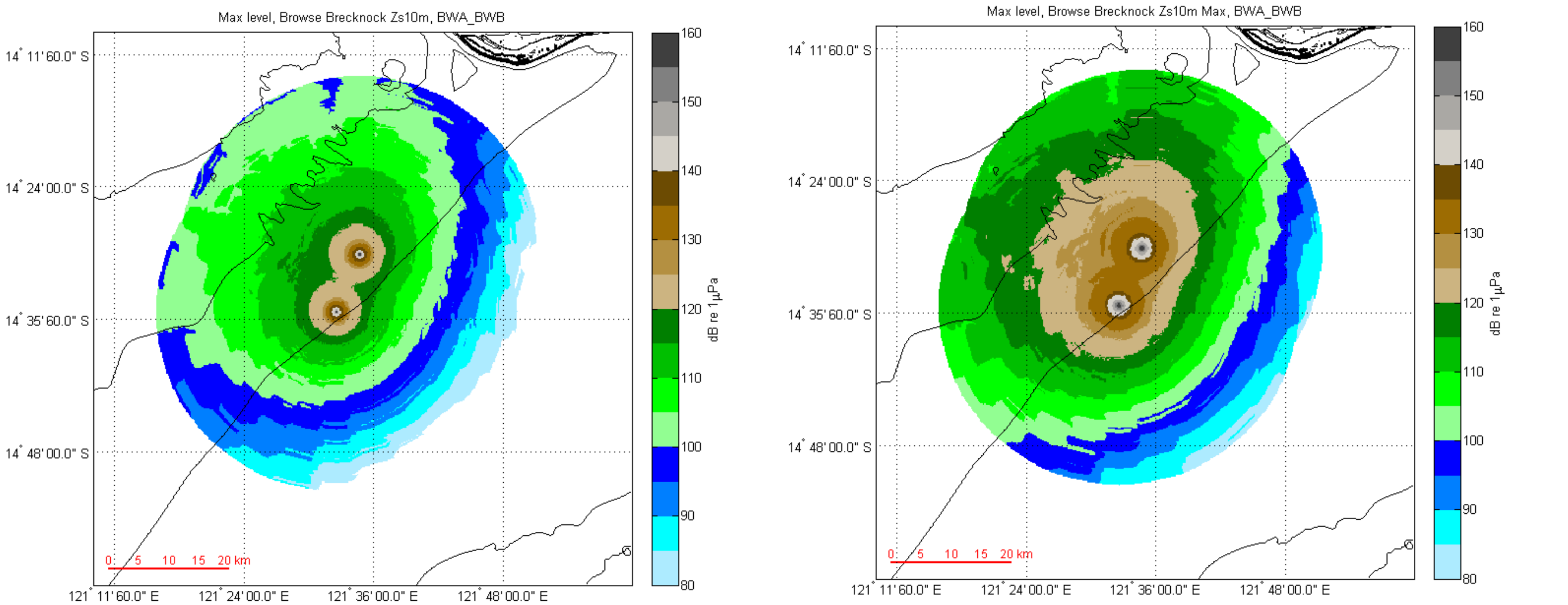

Figure 32. Scenario 6. Maximum received sound pressure level at any depth as a function of geographical position for normal FLNG operations at BWA and BWB. Left, calculations based on mean operational noise at both facilities. Right, calculations based on maximum operational noise at both facilities.

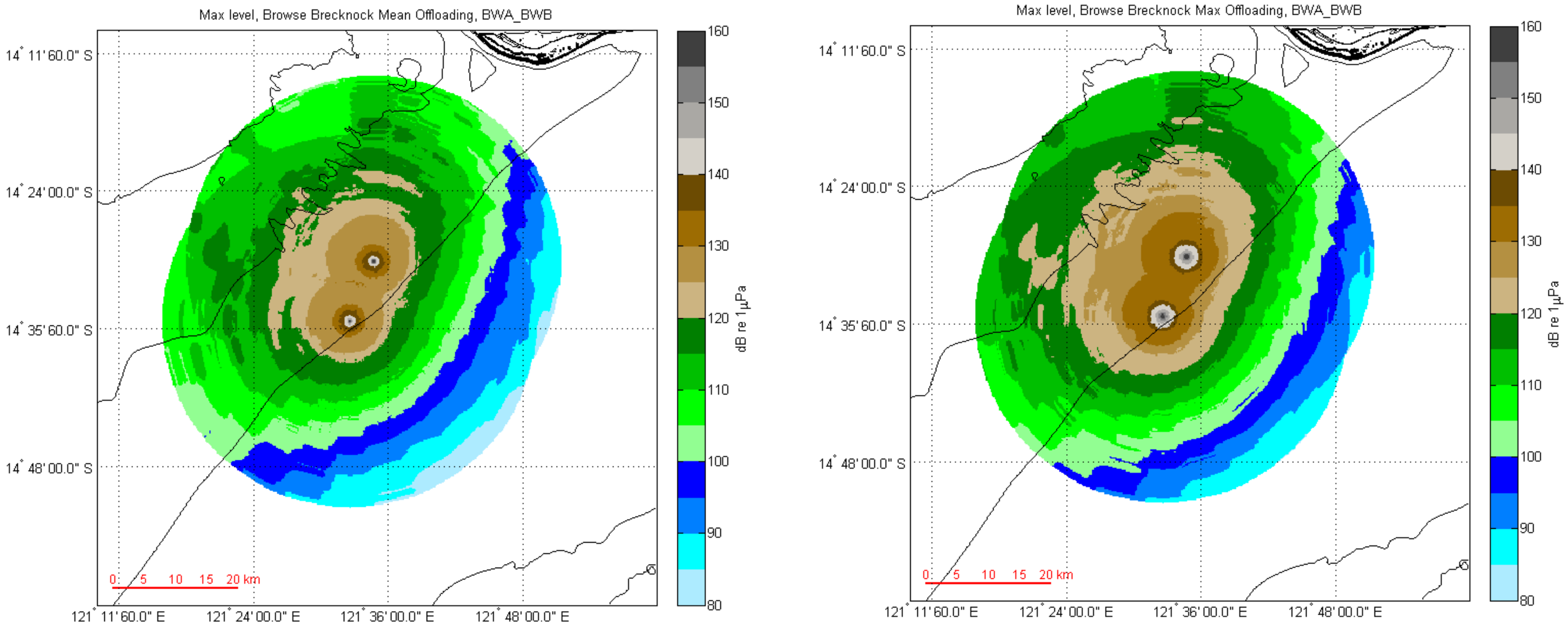

Figure 33. Scenario 7. Maximum received sound pressure level at any depth as a function of geographical position for FLNG offloading operations at both BWA and BWB. Left, calculations based on mean operational noise at both facilities. Right, calculations based on maximum operational noise at both facilities.

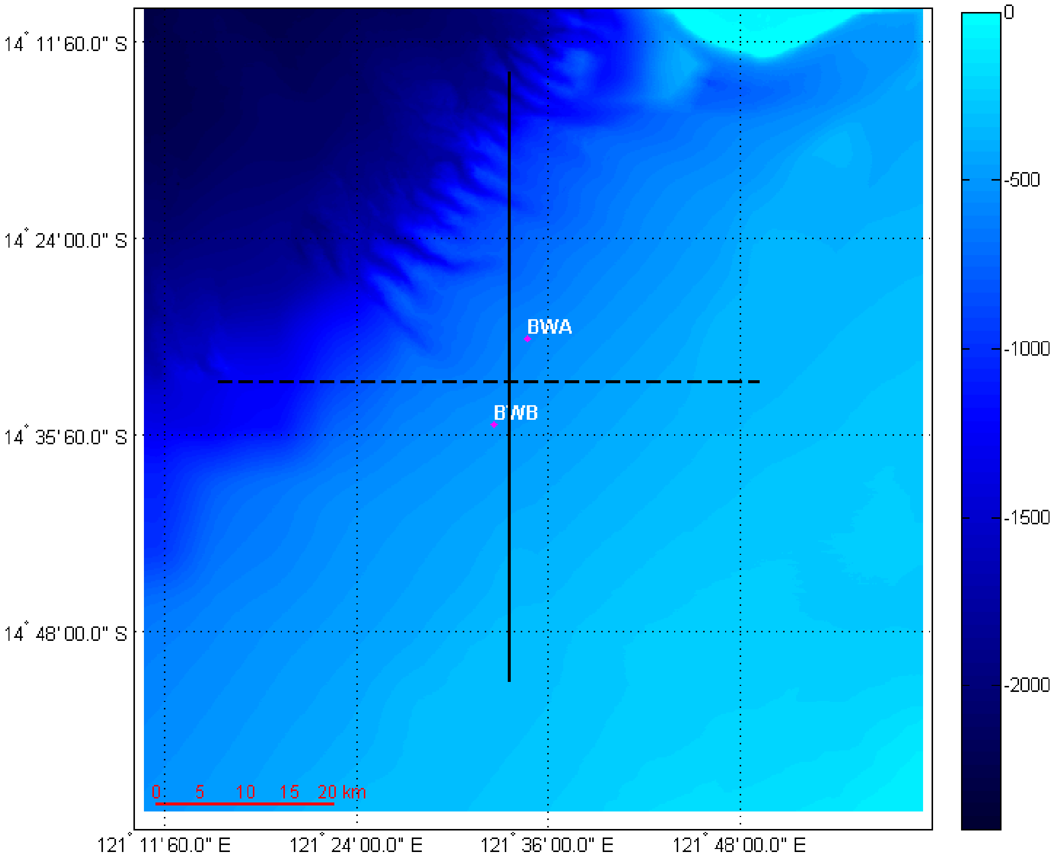

Figure 34. Locations of cross-sections through sound fields shown in the following plots.

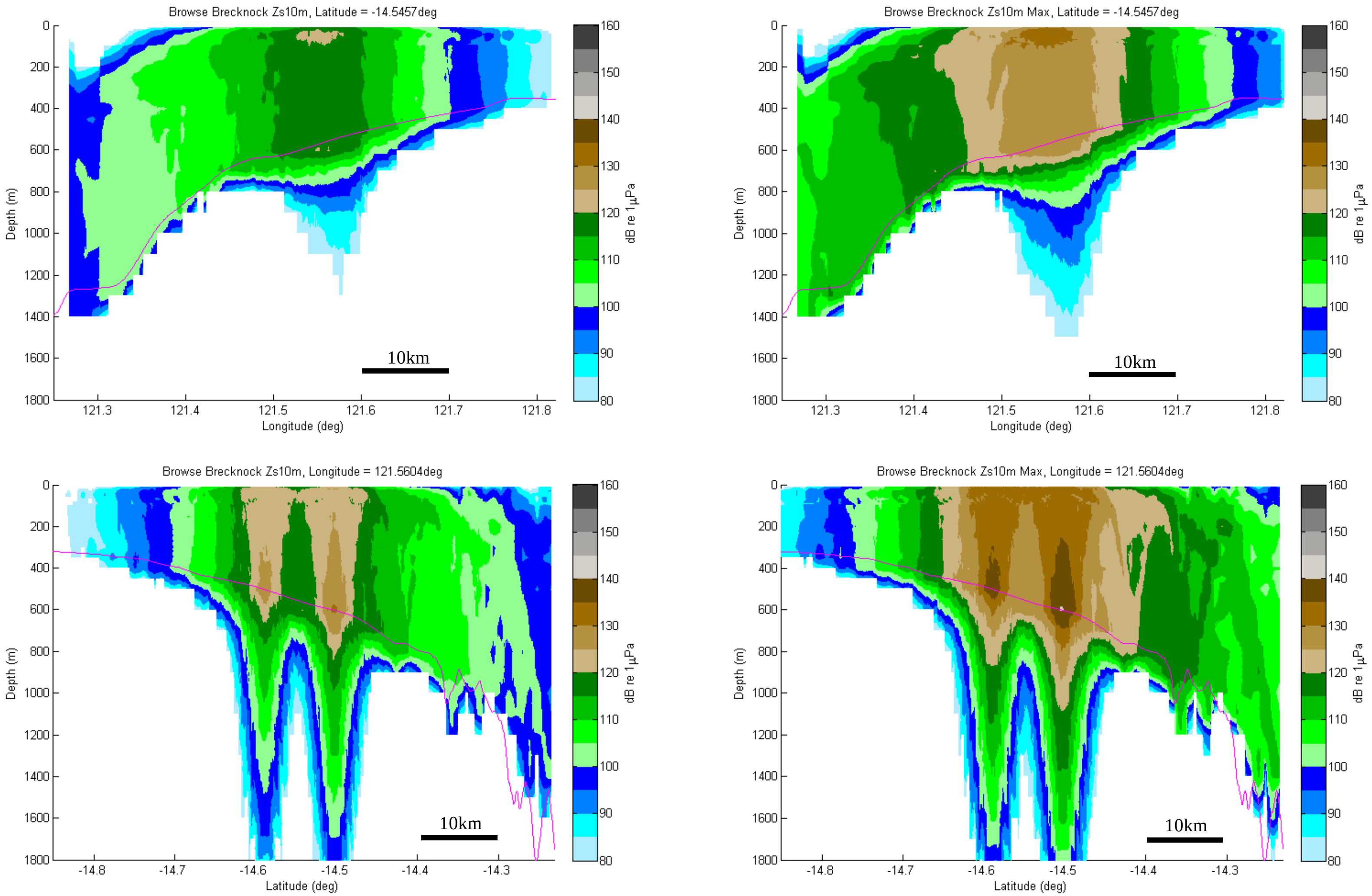

Figure 35. West-East (top) and South-North (bottom) cross sections through the gridded sound field for Scenario 6. Left hand plots are for mean FLNG operational noise, right hand plots are for maximum FLNG operational noise.

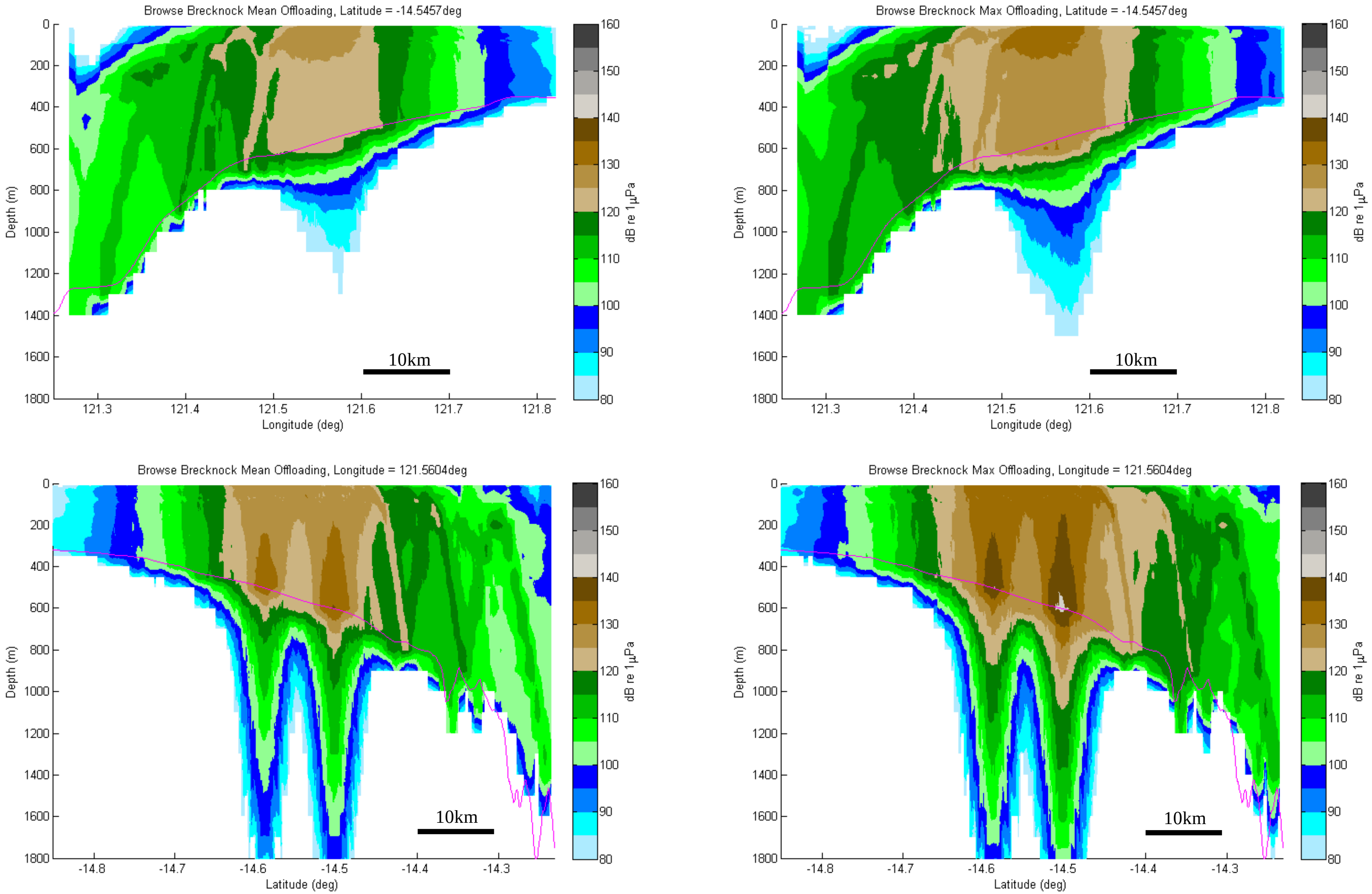

Figure 36. West-East (top) and South-North (bottom) cross sections through the gridded sound field for Scenario 7. Left hand plots are for offloading noise based on mean FLNG operational noise, right hand plots are for offloading noise based on maximum FLNG operational noise.

4 Conclusions

Received underwater noise levels from FLNG facilities operating in the Torosa and Brecknock/Calliance fields off north-western Australia have been modelled.

FLNG source spectra were estimated by scaling measured underwater noise spectra from existing Floating Production Storage and Offloading (FPSO) facilities, which indicated there would be an approximately 10 dB difference between mean and maximum noise levels from each FLNG facility during normal operations. The additional thruster cavitation noise present during offloading operations substantially increases the received noise levels above the mean FLNG operational noise, but only marginally increases it above the maximum FLNG operational noise.

The results show that sound from the Torosa facility is unable to penetrate into the North Reef lagoon but can penetrate the South Reef lagoon along some azimuths, due to the relatively deep sill along the northern boundary of this lagoon.

References

Fugro Survey (2004), “Geotechnical report, Montara Field development project offshore Timor Sea, Australia”, Fugro Survey Report P0080, August 2004.

Hamilton, E. L. (1980), “Geoacoustic modelling of the sea floor”, J. Acoust. Soc. America, 68 (5), Nov. 1980.

Jensen, F. B., Kuperman, W. A., Porter, M. B., Schmidt, H., *Computational Ocean Acoustics*, 2nd Ed., Springer, 2011, ISBN 978-1-4419-8677-1.

McCauley, R. D., "Radiated Underwater Noise Measured from the Drilling Rig *Ocean General*, Rig Tenders *Pacific Ariki* and *Pacific Frontier*, Fishing Vessel *Reef Venture*, and Natural Sources in the Timor Sea, Northern Australia". Centre for Marine Science and Technology Report C98-20, 1998.

Ross, D., *Mechanics of Underwater Noise*, Peninsula Publishing, 1987, ISBN 0-932146-16-3.

World Ocean Atlas (2005), NOAA National Oceanographic Data Centre, http://www.nodc.noaa.gov/OC5/WOA05/pr_woa05.html.